Biomass Conversion and Biorefinery (2024) 14:327–347
https://doi.org/10.1007/s13399-021-02285-0

ORIGINAL ARTICLE

Maximizing biomass productivity of cyanobacterium Nostoc sp. through high-throughput bioprocess optimization and application in multiproduct biorefinery towards a holistic zero waste

Jeeraporn Pekkoh[1,2,3,4] · Sureeporn Lomakool[1] · Jirayuth Chankham[1] · Kritsana Duangjan[2] · Theera Thurakit[1] · Kittiya Phinyo[1] · Khomsan Ruangrit[2] · Yingmanee Tragoolpua[1] · Chayakorn Pumas[1,2] · Wasu Pathom-aree[1,4] · Sirasit Srinuanpan[1,4]

Received: 30 September 2021 / Revised: 15 December 2021 / Accepted: 23 December 2021 / Published online: 10 February 2022

Abstract

This study aimed to maximize the biomass productivity of cyanobacterium *Nostoc* sp. AARL C008 by high-throughput bioprocess optimization, and to utilize the *Nostoc* biomass for application in multiproduct biorefinery towards holistic zero-waste technology. Through bioprocess optimization, maximum biomass productivity was obtained as 37.59 mg/L/day under modified BG-11 medium (0.190 g/L $K_2HPO_4{\cdot}3H_2O$, 0.0018 g/L citric acid and 2.53 mL/L trace metal solution) and continuous light feeding at 40 µmol/m^2/s. The zero-waste biorefining process was successfully used for *Nostoc* biomass to sequentially recover polysaccharides, phytochemicals, and lipids. *Nostoc* polysaccharides exhibited the bio-stimulant potential having the ability to improve soil properties such as moisture content, organic matter, microbiological activity, and cation exchange capacity by increases measured as 1.30, 1.55, 1.53, and 1.47-fold, respectively, compared to the control in which polysaccharides were absent. With 120 mg/L polysaccharides, the short length of melon was significantly enhanced 1.29-fold, higher than the control. After polysaccharide extraction, the cyanobacterial biomass residue (CBR) was used to extract the phytochemicals. *Nostoc* phytochemicals showed high antioxidant activity, giving ABTS activity of 26.10 mg TE/g-extract, DPPH activity of 5.71 mg GAE/g-extract, and PFRAP activity of 7.79 mg GAE/g-extract, as well as offering high-efficiency inhibitive effects on cancer cells with the IC_{50} recorded at 0.50 mg/mL. The CBR after phytochemical extraction can potentially be used to extract lipids prior to biodiesel production. The extracted lipid contained long-chain fatty acids with satisfactory fuel properties. The overall results evidenced that the multiproduct biorefining approach will make a significant contribution to the zero-waste industrialization of cyanobacterial-based bioproducts.

Keywords Cyanobacteria · Biomass · Biorefinery · Multiproduct · *Nostoc* · Bioprocess optimization

1 Introduction

The human population of our planet is expected to reach 9.7 billion by 2050, with the bulk of this growth coming from developing countries in Asia and Africa [1]. This rise in the global population is linked with an increase in the need for food and energy security in the future. Many countries are now looking for a sustainable supply of food and energy that does not endanger the environment. Cyanobacteria biomass is considered to be one of the most promising sources of future multiproduct due to its great multiplication rate and high-value components such as polysaccharides, lipids, pigments, and proteins [2]. Cyanobacteria are the among most numerous categories of microbes on the planet. They are autotrophic and may be found in a wide variety of

✉ Sirasit Srinuanpan
srinuanpan.s@gmail.com

1 Department of Biology, Faculty of Science, Chiang Mai University, Chiang Mai 50200, Thailand

2 Science and Technology Research Institute, Chiang Mai University, Chiang Mai 50200, Thailand

3 Environmental Science Research Center, Faculty of Science, Chiang Mai University, Chiang Mai 50200, Thailand

4 Research Center of Microbial Diversity and Sustainable Utilization, Faculty of Science, Chiang Mai University, Chiang Mai 50200, Thailand

environments, particularly in freshwater and marine settings. Several countries, especially in tropical areas, have successfully commercialized their use as food, feed, fertilizer, and hydrocolloids [1]. Nevertheless, only cyanobacterial *Spirulina* spp. are being cultivated on a massive scale with the majority of the produce destined for human use. In addition to *Spirulina*, *Nostoc* spp. is another well-known genus of cyanobacteria capable of fixing N_2 from the air for growth and accumulating carbohydrates (17–34% w/w), proteins (36–48% w/w), and phenolics (2–7% w/w) [3]. Found in Asia, particularly China, the Philippines, Thailand, Indonesia, Japan, and Taiwan, fresh *Nostoc* biomass is eaten raw as a salad. Although early studies indicate that *Nostoc* biomass has the potential to become a significant feedstock for the production of biofuels, biopolymers, pigments, food supplements, and biofertilizers [2], and this is still under development. Because of their challenging cultivation and economic unfeasibility, they have not been fully investigated on a commercial scale. Consequently, we have concentrated our efforts on investigating the use of *Nostoc* biomass to recover valuable sources of multiproducts.

Fostering a process that increases biomass productivity in relation to cyanobacteria-derived bioproducts and eliminating bottlenecks are key in promoting cultivation methods targeted at an industrial-scale profit. The major factors that restrict the biomass productivity of cyanobacteria are nutrient composition and concentration [4, 5], salinity stress responses [6], light penetration [7, 8], and the lack of light during the nighttime period [9]. The composition of macro- and micronutrients in the media, as well as their availability to cultures, have an impact on the cell development of cyanobacteria. Many media do not provide an optimal mix of macro- and micronutrients in the appropriate proportions. As a result of their non-toxicity to algal cells (nitrogen, potassium, magnesium, and sulfur), macronutrients such as these may be used in larger quantities. Essential micronutrients, on the other hand, such as iron, copper, manganese, zinc, cobalt, and molybdenum, are growth-limiting at low quantities and poisonous at excessive ones [10]. These micronutrients are essential in a variety of metabolic pathways that are involved in the cyanobacterial growth [4]. Furthermore, low nutrient concentrations limit the cell growth of microalgae and cyanobacteria, while higher concentrations induce substrate inhibition [4, 5]. Salinity is believed to be a regulating factor in the development of cyanobacteria in general since it has an effect on photosynthesis, the function of the plasma membrane, which in turn has an effect on cell growth. Apart from that, variations in salinity, as well as variations in turgor pressure on the cell, affect the shape and life cycle of cyanobacteria [6]. Light penetration is often poor inside photobioreactors, and the penetration decreases even more with increased cell density and depth owing to self-shading effects [7, 8]. Light/dark cycles are also necessary for cyanobacteria growth, and it has been observed that the respiratory action of cyanobacteria at night causes a reduction in biomass generated during the daytime [9]. Even though many researchers have worked hard to address the present issues of poor biomass productivity, further research and development are still required since the optimum growth varies depending on the strain cultivated. Therefore, high-throughput bioprocess optimization of nutrient composition and concentration and key physicochemical parameters needs to be pursued for obtaining higher productivity of cyanobacterial biomass that will help to ensure the long-term commercial development of cyanobacteria-based bioproducts.

Despite the fact that cyanobacteria have great potential to become the main actors in alternative renewable feedstocks, many production processes of chemicals from cyanobacterial biomass have been concentrated on a single product, with most of the current research focusing on biofuels [11]. More recently, cascading bio-refineries are being explored in order to maximize the intrinsic value of all components contained in the cyanobacterial biomass. For example, Shahid et al. [2] developed an integrated process that was applied to four cyanobacteria, including *Acaryochloris marina* BERC03, *Oscillatoria* sp., BERC04, and *Pleurocapsa* sp. BERC06 and sequentially recovered phycobilins as high-valued pigments/phytochemicals having bioactivities and lipids as a promising feedstock for biodiesel, as two fractions of economic importance. During the biomass utilization, an unavoidable amount of biomass residual waste is produced, which is a contaminant to the environment and increases the cost of disposal. Also possible is the valorization of biomass residual waste into value-added products such as polysaccharide biostimulant-based products [12]. It has been reported that cyanobacteria biomass that has been de-oiled and depigmented is mostly composed of carbohydrates and proteins, and it may be used to produce bioethanol and useful enzymes via fermentation [2]. In addition, polysaccharide and protein-rich biomass may be utilized for a variety of purposes, including biological or thermochemical conversion to bio-oil, biochar, and syngas, as well as usage as an animal feed additive for a variety of animal species [1]. Ruangrit et al. [13] suggested that creating a profitable and competitive multiproduct from biomass through the integrated production of additional gainful value-added components that have a demonstrated market worth should be investigated in order to utilize macroalgae while minimizing waste generation. A zero-waste biorefining process is a feasible and appropriate approach that could maximize the utilization of cyanobacterial biomass for chemical multiproduction along with the required properties [2]. Despite the fact that there have been many studies on the biorefinery of cyanobacterial biomass, none of these have evaluated the use of *Nostoc* biomass for the integrated production of

bio-stimulant polysaccharides, bioactive phytochemicals, and biodiesel with the desired properties.

Therefore, this study aimed to maximize the biomass productivity of *Nostoc* sp. AARL C008 through the high-throughput bioprocess optimization of medium components and concentration. Key physiochemical factors (namely salinity, light intensity, and photoperiod) were also optimized. The resulting *Nostoc* biomass was then used to sequentially recover polysaccharides, phytochemicals, and lipids using a zero-waste biorefining process for the multi-production of bio-stimulants, bioactive chemicals, and biodiesel. Firstly, the *Nostoc* biomass was hot-water extracted and partially purified by alcohol precipitation to recover water-soluble polysaccharides (WSP). *Nostoc* WSP was characterized to evaluate the ability to improve soil properties and the potential for plant growth promotion using green net melon as a plant model. After polysaccharide extraction, polysaccharide-free residual powdered biomass (PRPB) was used to extract the phytochemicals. The chlorophylls, carotenoids, and total phenolics of *Nostoc* phytochemicals were determined. Antioxidant activity, including DPPH and ABTS radical scavenging activity, and potassium ferricyanide reducing antioxidant power (PFRAP) activity, and antiproliferative properties on human skin cancer cells were also evaluated. Lastly, polysaccharide-free and phytochemical-free residual powdered biomass (PPRPB) was used to extract lipids prior to acid-catalyzed transesterification for biodiesel production. The fatty acid composition of the obtained *Nostoc* lipid and fuel qualities of the produced biodiesel were estimated. This research will also offer results that will add to the existing knowledge in databases concerned with the zero-waste industrialization of cyanobacterial-based bioproducts.

2 Materials and methods

2.1 Cyanobacteria

Pure culture of cyanobacterium *Nostoc* sp. AARL C008 was obtained from the Applied Algal Research Laboratory (AARL), Department of Biology, Faculty of Science, Chiang Mai University, Thailand. The culture was precultured in BG-11 medium [14] under 25 ± 1 °C and continuous illumination with fluorescent lamp at 31.97 µmol/m^2/s for 30 days. The BG-11 medium contained 1.5 g $NaNO_3$, 0.04 g $K_2HPO_4{\cdot}3H_2O$, 0.075 g $MgSO_4{\cdot}7H_2O$, 0.036 g $CaCl_2{\cdot}2H_2O$, 0.006 g citric acid, 0.006 g Fe ammonium citrate, 0.001 g Na_2EDTA-Mg, 0.02 g Na_2CO_3, and 1 mL of trace metal solution per liter, pH 7.4. The trace metal solution contained 2.86 g H_3BO_3, 1.81 g $MnCl_2{\cdot}4H_2O$, 0.222 g $ZnSO_4{\cdot}7H_2O$, 0.079 g $CuSO_4{\cdot}5H_2O$, 0.049 g $CoCl_2{\cdot}6H_2O$, and 0.39 g $Na_2MoO_4{\cdot}2H_2O$ per liter.

2.2 Maximizing biomass productivity of cyanobacterium Nostoc sp. AARL C008

2.2.1 Medium optimization

Experiment for medium optimization of *Nostoc* sp. AARL C008 cultivation was conducted in 250 mL Erlenmeyer flask with 200 mL BG-11 medium and the initial cells concentration of 0.30 ± 0.04 g/L under 25 ± 1 °C and continuous illumination with fluorescent lamp at 40 µmol/m^2/s for 15 days. Optimizations of the BG-11 medium was performed through Plackett–Burman Design (PBD) as a first optimization step to identify which nutrient components have a significant effect on biomass productivity of *Nostoc* sp. AARL C008. In this study, the nine variables in the medium components (A: $NaNO_3$, B: $K_2HPO_4{\cdot}3H_2O$, C: $MgSO_4{\cdot}7H_2O$, D: $CaCl_2{\cdot}2H_2O$, E: citric acid, F: Fe ammonium citrate, G: Na_2EDTA-Mg, H: Na_2CO_3, and I: trace metal) were screened in twelve experimental designs. Each variable was evaluated at two levels – for the low level and + for the high level. The design is shown in Table 1, and the given biomass productivity were the average of three replications. The design was based on the following first-order polynomial model (Eq. 1) and the effect of each variable was determined using Eq. 2.

$$Y = \beta_0 + \sum \beta_i x_i \tag{1}$$

$$E_{(X_i)} \frac{2\,(\sum M_{i+} - \sum M_{i-})}{N} \tag{2}$$

where Y is the dependent variable (biomass productivity), namely the biomass productivity. β_0 is the constant coefficient/the model intercept/the of set term. β_i is the linear effect. x_i is the independent variable (factors). $E_{(X_i)}$ is the standardized effect of the tested variable, M_{i+} and M_{i-} are the responses from trials where the variable (x_i) is presented at high and low levels, respectively, and N is the number of experimental runs.

The significant variables from PBD analysis were subsequently optimized through Response Surface Methodology (RSM) using the Central Composite Design (CCD) with five levels to maximize the biomass productivity, leading to 17 runs, consisting of eight factorial points, six axial points, and three central points. The design is shown in Table 3, and the given biomass productivity were the average of three replications from independent cultivation. The design was based on the following second-order polynomial model (Eq. 3).

$$Y = \beta_0 + \sum \beta_i x_i + \sum \beta_{ii} x_i^2 + \sum \beta_{ij} x_i x_j \tag{3}$$

where Y is the experimental response (biomass productivity), x_i and x_j represent the variables or parameters, β_0 is the offset term, β_i is the linear effect, β_{ij} is the first order

Table 1 Plackett–Burman design variables (in coded levels) for biomass productivity

Run	A	B	C	D	E	F	G	H	I	Biomass productivity (mg/L/day)
1	+	−	+	−	−	−	+	+	+	12.41 ± 0.63
2	+	+	−	+	−	−	−	+	+	18.15 ± 5.60
3	−	+	+	−	+	−	−	−	+	21.77 ± 0.33
4	+	−	+	+	−	+	−	−	−	9.81 ± 1.49
5	+	+	−	+	+	−	+	−	−	29.74 ± 0.72
6	+	+	+	−	+	+	−	+	−	33.03 ± 1.04
7	−	+	+	+	−	+	+	−	+	19.42 ± 0.36
8	−	−	+	+	+	−	+	+	−	18.20 ± 1.56
9	−	−	−	+	+	+	−	+	+	17.52 ± 2.04
10	+	−	−	−	+	+	+	−	+	18.04 ± 1.65
11	−	+	−	−	−	+	+	+	−	36.44 ± 0.81
12	−	−	−	−	−	−	−	−	−	12.52 ± 1.61

interaction effect, and β_{ii} is the squared effect. The goodness of the fit of the model was evaluated by the coefficient of determination (R^2) and the analysis of variance (ANOVA). Response surface plots were developed to indicate an optimum condition using the fitted quadratic polynomial equations obtained by holding one of the independent variables at a constant value and changing the levels of the other two variables.

2.2.2 Optimizing physicochemical factors

The *Nostoc* sp. AARL C008 were cultivated in optimized BG-11 medium obtained from above experiments under different salinities of 1.1 as the control, 4.6, 8.1, 15.1, 29.1, 57.1, and 91.1 ppt, different light intensities of 25, 40, 50, 75, and 100 µmol/m^2/s and different photoperiods of 12:12, 16:8 and 24:0 h light and dark cycles at the same conditions as mentioned above. The biomass productivity was evaluated.

2.2.3 Determination of biomass productivity

The *Nostoc* sp. AARL C008 biomass was harvested using centrifugation at 6000 rpm for 15 min and the pellets were washed with distilled water twice and were then dried at 60 °C until constant weight. The biomass productivity was calculated using the following equation (Eq. 4).

$$P_{\text{biomass}} = (X_t - X_0)/(t - t_0) \quad (4)$$

where P_{biomass} is biomass productivity (mg/L/day), X_t is the biomass concentration (mg/L) at time t (day) and X_0 at time $t = 0$ d (t_0).

2.3 Extraction of polysaccharides and their biostimulants potential

2.3.1 Polysaccharide extraction

Extraction of polysaccharide from cyanobacterium *Nostoc* sp. AARL C008 biomass was performed according to Ruangrit et al. [13] method with minor modifications. Briefly, dried biomass (10 g) was mixed with distilled water (1 L) at 98 °C for 1 h. The mixture was centrifuged at 6000 rpm for 15 min and the pellet was continually extracted twice times. The extract was then concentrated and submitted to graded precipitation with 95% ethanol (1:2 v/v) and the mixture was kept overnight at 4 °C, then centrifuged at 6000 rpm for 20 min, and dried at 60 °C until constant weight to obtain crude polysaccharide (CPS). Total sugar content and reducing sugar content of CPS were determined by phenol–sulfuric acid method [15] and DNS method [16], respectively. The monosaccharide composition of CPS was analyzed by high-performance liquid chromatography (HPLC) (UFLC, Shimadzu, Japan) with a Shodex VG-50 4E column as described previously [13]. The functionalization of CPS was identified by attenuated total reflectance–Fourier transform infrared spectrometry (ATR–FTIR, Thermo Scientific Nicolet iS50) by varying wavenumbers from 400 to 4000 cm^{-1} with a resolution of 4 cm^{-1}. The ^{1}H-NMR spectra of CPS was analyzed by dissolving 6 mg of CPS in 400 µL of D_2O. The solution was stirred for 2 h at 40 °C before being lyophilized. The process was repeated two more times. The

lyophilized CPS was dissolved in 600 µL D_2O, placed in an NMR tube, and subjected to a Bruker 500 MHz NMR.

2.3.2 Evaluation of soil improvement ability

The soil improvement ability of cyanobacterial CPS was determined following the methods of Tiche et al. [17] with some modifications. Briefly, soil sample obtained from Faculty of Agriculture, Chiang Mai University, Thailand was mixed with the CPS at the concentration of 120 mg CPS/kg soil and were then immersed in tap water for 15 days in the greenhouse before evaluation of soil properties. Changes in soil properties including soil moisture [18], organic matter [19], soil microbial activity [20], and cation exchange capacity [21] were analyzed.

2.3.3 Evaluation of plant growth promotion potential

The potential use of CPS to promote plant growth was tested using green net melon as a plant model. The germinated melon seeds (5 days old) were grown for 4 weeks in pots containing 1 kg soil and five pots received 3 germinated seeds. The plants were maintained under greenhouse conditions (12 h photoperiod, 230–740 µmol/m^2/s photosynthetically active radiation, 18–38 °C temperature range, 16–71% relative humidity range) and were watered daily with 300 mL of water. A 300 mL of CPS (at concentration of 0, 60, 120, and 240 mg/L) were weekly added. After 4 weeks of growth, the length was recorded and changes in total number of bacteria, fungi, and actinomycetes were also determined using serial dilution spread plate method [22].

2.4 Phytochemical extraction and their bioactivities

2.4.1 Extraction of phytochemicals

The polysaccharide-free residual powdered biomass (PRPB) (2.5 g) obtained from Sect. 2.3 was extracted using ethyl acetate:methanol (1:1 v/v, 100 mL) by incubation at 4 °C for 24 h [23]. The mixture was then centrifuged at 6000 rpm and 4 °C for 5 min. The obtained pellets were continually extracted until colorless and the supernatant was collected and subjected to the UV–Vis spectrophotometer (250–700 nm). The sample was then evaporated to dryness in a rotary-evaporator under reduced pressure at 40 °C before bioactivity evaluation.

2.4.2 Determination of DPPH radical scavenging activity

The DPPH radical scavenging activity was determined according to the method described by Pekkoh et al. [24] with minor modifications. A 50 µL aliquot of 1.3 mM DPPH dissolved in methanol was mixed with 100 µL of the sample solution (the tested concentration at 0.2–12.5 mg/mL) in a 96-well plate. The radical stock solution was freshly prepared. The mixture was incubated for 30 min in dark condition at room temperature. The absorbance of DPPH was measured at 517 nm. Gallic acid was used as the reference standard (Supplementary data) and the following equation (Eq. 5) was used to determine the scavenging activity (%).

$$\text{DPPH radical scavenging activity} = [(A_{control} - A_{sample})/A_{control}] \times 100 \quad (5)$$

where $A_{control}$ is the absorbance of the control reaction (distilled water instead of the sample was used as control) and A_{sample} is the absorbance of the sample. The DPPH activity was reported as gallic acid equivalent (GAE) per g extract.

2.4.3 Determination of ABTS radical scavenging activity

The ABTS radical scavenging activity was determined following a modified Ruangrit et al. [13] method. The ABTS solution was prepared by mixing 7 mM ABTS solution with 2.45 mM potassium persulfate (final concentration). The mixture was incubated for 12–16 h in dark condition at room temperature. Then, the absorbance at 734 nm of the ABTS solution was adjusted to 0.700 ± 0.020 using deionized water. A 5 µL aliquot of the sample solution (the tested concentration at 0.2–25.0 mg/mL) was mixed with 195 µL of the ABTS solution in a 96-well plate. The mixture was incubated for 10 min at 37 °C and the reduction of ABTS was measured at 734 nm using a 96-well plate reader. Trolox was used as the reference standard (Supplementary data) and the following equation (Eq. 6) was used to determine the scavenging activity (%).

$$\text{ABTS radical scavenging activity} = [(A_{control} - A_{sample})/A_{control}] \times 100 \quad (6)$$

where $A_{control}$ is the absorbance of the control reaction (distilled water instead of the sample was used as control) and A_{sample} is the absorbance of the sample. The ABTS activity was reported as Trolox equivalent (TE) per g extract.

2.4.4 Determination of potassium ferricyanide reducing antioxidant power activity

The PFRAP assay was determined following the methods of Lomakul et al. [25] with some modifications. A 130 µL aliquot of the sample solution (the tested concentration at $0.2 - 50.0$ mg/mL) was mixed with 290 µL of 0.2 M sodium phosphate buffer (pH 6.6) and 290 µL of 1% potassium ferricyanide. The mixture was incubated for 20 min at 50 °C. After 290 µL of 10% (w/v) trichloroacetic acid was added, the mixture was centrifuged at 3000 rpm for 10 min. The supernatant solution (1 mL) was mixed with 1 mL of distilled water and 200 µL of 0.1% ferric chloride.

The absorbance was measured at 700 nm and gallic acid was used as the reference standard. The PFRAP activity was reported as gallic acid equivalent (GAE) per gram extract.

2.4.5 Determination of anticancer activity

The cytotoxicity of the methanolic extracts on Vero cells and malignant melanoma cells (A375 skin cancer cells) was tested using the MTT assay as described by Umthong et al. [26]. Briefly, 10^5 cell/mL of Vero cells and A375 cells were placed into 96-well plates and incubated for 24 h at 37 °C in a 5% CO_2 incubator. After the cell incubation, each concentration of samples (the tested concentration at 0.4–2.5 mg/mL) was treated with Vero cells or A375 cells and incubated for 48 h at 37 °C in a 5% CO_2 incubator. Then, 2 mg/mL MTT solution (Bio Basic Inc., Markham, ON, Canada) was added and the resulting mixture was incubated for 4 h. The absorbance was measured at 540 and 630 nm. The percentage of cell viability and 50% inhibitory concentration (IC_{50}) were calculated.

2.5 Extraction of lipids and their biodiesel production

2.5.1 Extraction of lipid

Extraction of lipid from polysaccharide-free and phytochemical-free residual powdered biomass (PPRPB) was performed according to Ruangrit et al. [13] method with minor modifications. Briefly, dried PPRPB (100 mg) was extracted 10 mL CH_2Cl_2/MeOH (2:1 v/v) and sonicated with sonicator (40 kHz) at room temperature with extracted twice times. The extracted lipids were centrifuged to obtain a clear supernatant, and the solvent was removed by feeding nitrogen gas stream. The extracted lipid was dried and weighed. The lipid content was calculated as percentage of lipid to PPRPB.

2.6 Fatty acid and biodiesel compositional analysis

The extracted lipid was converted to fatty acid methyl esters (FAMEs) by acid-catalyzed transesterification [27]. The extracted lipid sample (10°mg) was mixed with 0.5 mL toluene, 1.5 mL of methanol, and 50 µl of 35% conc. HCl and the mixtures were then incubated at 98 °C for 2 h. After cooling, 1 mL of hexane was added and vortexed. The hexane layer (FAME) was collected prior to analyzing the FAMEs composition using a 7890B Gas Chromatograph equipped with a cross-linked capillary HP-5 column (length 30 m, 0.32 mm I.D, 0.25-µm film thickness) and a flame ionization detector. Operating conditions were as follows: inlet temperature at 230 °C, initial oven temperature at 45 °C held for 2 min, then ramped to 100 °C at 25 °C/min, held for 4 min, then ramped to 200 °C at 5 °C/min, held for 8 min, then ramped to 250 °C at 5 °C/min, held for 6 min, and the detector temperature at 230 °C. The fatty acids were identified by comparing their retention times with known pure standards. The fatty acid profiling was used to calculate the biodiesel properties of macroalgae such as saponification value (SV, mg KOH/g), iodine value (IV, g I_2/100 g), cetane number (CN), degree of unsaturation (DU, %wt), long-chain saturated factor (LCSF, %wt), cold filter plugging point (CFPP, °C), high heating value (HHV, MJ/kg), cloud point (CP, °C), kinematic viscosity (υ, ln KV at 40 °C in mm^2/s), density (ρ, g/cm^3), oxidative stability (OS; h), allylic position equivalents (APE), bis-allylic position equivalents (BAPE), and oxidation stability index (OSI, h at 110 °C) using empirical Eqs. (7)–(20) reported by Srinuanpan et al. [27], Talebi et al. [28], and Patel et al. [29].

$$SV = \sum[(560 \times F)/MW] \tag{7}$$

$$IV = \sum[(254 \times F \times D)/MW] \tag{8}$$

$$CN = [46.3 + (5458/SV)] - (0.225 \times IV) \tag{9}$$

$$DU = \%MUFA + (2 \times \%PUFA) \tag{10}$$

$$LCSF = (0.1 \times C16) + (0.5 \times C18) + (1 \times C20) + (1.5 \times C22) + (2 \times C24) \tag{11}$$

$$CFPP = (3.1417 \times LCSF) - 16.477 \tag{12}$$

$$HHV = 49.43 - (0.041 \times SV) - (0.015 \times IV) \tag{13}$$

$$CP = (0.526 \times C16) - 4.992 \tag{14}$$

$$\upsilon = -12.503 + 2.496 \times \ln(\sum MW) - 0.178 \times \sum D \tag{15}$$

$$\rho = 0.8463 + 4.9/\sum MW + 0.0118 \times \sum DB \tag{16}$$

$$OS = 117.9295/(\%C18{:}2 + \%C18{:}3) + 2.5905 \tag{17}$$

$$APE = (\%C18:1 + \%C18:2 + \%C18:3) \times 2 \tag{18}$$

$$BAPE = (2 \times \%C18:3) + \%C18:2 \tag{19}$$

$$OSI = 3.91 - (0.045 \times BAPE) \tag{20}$$

where D is the number of double bonds, F is the % of each type of fatty acid, MW is the molecular weight of corresponding fatty acid, MUFA is the weight percentage of

the monounsaturated fatty acids (wt%), PUFA is the weight percentage of the polyunsaturated fatty acids (wt%).

2.7 Statistical analysis

All experiments for the same experimental condition were performed in triplicates. The results are expressed as mean plus standard deviations. Analysis of variance was performed to evaluate significant differences in treatment means, and the least significant difference was used to separate means, using SPSS software.

3 Results and discussion

3.1 Maximizing biomass productivity of cyanobacterium Nostoc sp. AARL C008

3.1.1 Optimization of medium components

Screening of the significant nutrient components using Plackett–Burman design In this study, the Plackett–Burman design (PBD) was used for the screening of variables as nutrient components strongly influencing the biomass productivity of cyanobacterium *Nostoc* sp. AARL C008. Twelve experimental runs for biomass productivity with combinations of the two levels of each variable were performed as shown in Table 1. The biomass productivities were found to range between 9.81 and 36.44 mg/L/day, indicating a significant variance in the biomass production. Through the analysis of the regression model (ANOVA) as presented in Table 2, three nutrient components that had a significant effect on the biomass productivity were $K_2HPO_4{\cdot}3H_2O$, citric acid, and trace metal with a high confidence value (> 95%) and low *P*-value (< 0.05), while the six others, namely $NaNO_3$, $MgSO_4{\cdot}7H_2O$, $CaCl_2{\cdot}2H_2O$, Fe ammonium citrate, Na_2EDTA-Mg, and Na_2CO_3 showed insignificant effects on the biomass productivity (Table 2). According to the contribution percentages, the important degrees of influence by the three significant nutrient components on the biomass productivity were as follows: $K_2HPO_4{\cdot}3H_2O$ > trace metal > citric acid. It was also discovered that $K_2HPO_4{\cdot}3H_2O$ and citric acid gave a positive effect on the biomass productivity with standardized effects of 11.61 and 4.93, respectively. These positive effects mean that if the concentrations of $K_2HPO_4{\cdot}3H_2O$ and citric acid are increased, the biomass productivity can also be increased. Meanwhile, trace metal had a negative effect (standardized effect of − 5.40) on the biomass productivity, which means that if a lower trace metal solution was added, the biomass productivity could be improved. Similar results have been reported by Luo et al. [30] who found that the addition of $K_2HPO_4{\cdot}3H_2O$, citric acid, and trace elements enhanced the biomass productivity of microalga *Scenedesmus* sp. L-1 grown in BG-11 medium.

In the literature, $K_2HPO_4{\cdot}3H_2O$ functioning like a source of phosphorus is necessary to cyanobacterial cells for the production of cellular components such as phospholipids, DNA, RNA, and ATP for the metabolic pathways involving energy transfer and nucleic acid synthesis [31]. Meanwhile, citric acid solubilizes the salts, preventing precipitation, and therefore increases cell availability leading to a faster growth rate [10]. Zabochnicka-Swiątek et al. [32] reported that the role of citric acid is crucial for improving the bioavailability of iron in the nutrient solution. Citric acid also maintains the pH of the culture medium and serves as a source of energy for the developing cells, while trace metal solution acts as a co-factor for key enzymes involved in respiration and photosynthesis [4]. Other nutrient components were also of great benefit for cyanobacteria, as reported by Markou et al. [33]. In particular, nitrogen plays the most important role in the growth of cyanobacteria; a rise in the nitrogen concentration leads to an increase in the growth and biomass production of cyanobacteria [34]. However, based on the results (Table 2), nitrogen was

Table 2 Level of the variables and statistical analysis (ANOVA) of Plackett–Burman design for biomass productivity

Variables	Code	Low level (−)	High level (+)	Coefficient	Effect	*P*-value	Confidence (%)	Contribution (%)	Significance
$NaNO_3$ (g/L)	A	0.3	7.5	− 0.39	− 0.78	0.52	48	0.24	Insignificant
$K_2HPO_4{\cdot}3H_2O$ (g/L)	B	0.008	0.2	5.84	11.67	0.01	99	53.66	Significant
$MgSO_4{\cdot}7H_2O$ (g/L)	C	0.015	0.375	− 1.48	− 2.96	0.10	90	3.46	Insignificant
$CaCl_2{\cdot}2H_2O$ (g/L)	D	0.0072	0.18	− 1.78	− 3.56	0.07	93	4.99	Insignificant
Citric acid (g/L)	E	0.0012	0.03	2.46	4.93	0.04	96	9.55	Significant
Fe ammonium citrate (g/L)	F	0.0012	0.03	1.79	3.58	0.07	93	5.04	Insignificant
Na_2EDTA-Mg (g/L)	G	0.0002	0.005	1.79	3.58	0.07	93	5.03	Insignificant
Na_2CO_3 (g/L)	H	0.004	0.1	2.04	4.08	0.06	94	6.53	Insignificant
Trace metal (mL/L)	I	0.2	5	− 2.70	− 5.40	0.03	97	11.50	Significant

Table 3 Central composite design with the experiment response

Run	$K_2HPO_4{\cdot}3H_2O$ (g/L)	Citric acid (g/L)	Trace metal (mL/L)	Biomass productivity (mg/L/day)	
				Experiment value	Predicted value
1	0.008	0.0012	0.2	13.63±0.26	15.35
2	0.200	0.0012	0.2	33.87±0.09	34.76
3	0.008	0.0300	0.2	18.53±0.33	20.48
4	0.200	0.0300	0.2	27.80±0.14	28.46
5	0.008	0.0012	5.0	15.07±0.05	18.17
6	0.200	0.0012	5.0	36.43±0.31	38.25
7	0.008	0.0300	5.0	14.27±0.19	17.14
8	0.200	0.0300	5.0	23.73±0.19	25.78
9	0.000	0.0156	2.6	12.23±0.16	8.31
10	0.265	0.0156	2.6	33.30±0.21	31.90
11	0.104	0.0000	2.6	34.27±0.19	31.60
12	0.104	0.0398	2.6	28.10±0.07	25.44
13	0.104	0.0156	0.0	27.93±0.05	26.64
14	0.104	0.0156	6.6	30.80±0.14	26.76
15	0.104	0.0156	2.6	30.67±0.24	30.24
16	0.104	0.0156	2.6	28.07±0.05	30.24
17	0.104	0.0156	2.6	31.07±0.05	30.24

Noted: Low Medium High

an insignificant factor for biomass productivity. This might be due to the sufficient nitrogen level required for *Nostoc* sp. growth. One of the possible reasons is that cyanobacteria *Nostoc* are capable of nitrogen fixation from the air for their growth and biomass production [3]. Marino and Howarth [35] suggested that the most suitable conditions seem comparable to those of natural freshwater, such as low availability of inorganic nitrogen and high levels of phosphorus.

Optimization using Central Composite design Based on the Plackett–Burman design, three important nutrient components including $K_2HPO_4{\cdot}3H_2O$ (A), citric acid (B), and trace metal solution (C) were then optimized by the RSM approach with Central Composite design (CCD) to obtain the maximum productivity of *Nostoc* sp. AARL C008 biomass (Y). The observed and predicted responses in biomass productivity are presented in Table 3. The biomass productivity ranged from 12.23 to 36.43 mg/L/day, and the lowest and highest concentrations of biomass productivity were found in runs 9 and 6, respectively. The biomass productivity was significantly dependent on the $K_2HPO_4{\cdot}3H_2O$ concentration. When using a low concentration of $K_2HPO_4{\cdot}3H_2O$, the biomass productivity was limited at 12.23–18.53 mg/L/day (Run 1, 3, 5, 7, and 9, while using a high $K_2HPO_4{\cdot}3H_2O$ concentration resulted in the biomass productivity reaching as high as > 23 mg L^{-1} day^{-1} (Run 2, 4, 6, 8, and 10). Through CCD, the second-order polynomial model was applied to determine the relationship between the biomass productivity of *Nostoc* sp. AARL C008 and test the nutrient components as follows (Eq. 21):

Table 4 ANOVA for response surface quadratic model of response variance

Source	SS	Df	MS	*F*-value	*P*-value
Model	950.36	9	105.6	8.36	0.01*
A-$K_2HPO_4{\cdot}3H_2O$	671.5	1	671.5	53.16	0.00*
B-Citric acid	45.9	1	45.9	3.63	0.10
C-Trace metal	0.017	1	0.017	1.38×10^{-3}	0.97
AB	65.36	1	65.36	5.17	0.06
AC	0.22	1	0.22	0.018	0.90
BC	19.01	1	19.01	1.51	0.26
A^2	144.7	1	144.7	11.46	0.01*
B^2	4.15	1	4.15	0.33	0.58
C^2	17.59	1	17.59	1.39	0.28
Residual	88.42	7	12.63		
Lack of fit	83.11	5	16.62	6.26	0.14
Pure error	5.31	2	2.65		
Cor total	1038.77	16			
R^2	0.91				
CV	13.74				

*significant within a 95% confidence interval, *SS* sum of square, *Df* degree of freedom, *MS* mean square, R^2 regression coefficient, *CV* coefficient of value

$$Y = 13.24 + 184.28A + 295.02B + 1.76C - 2.07\times10^{3}AB + 0.72AC - 44.61BC - 388.74A^2 - 2.93\times10^{3}B^2 - 0.22C^2 \quad (21)$$

where Y = biomass productivity (mg/L/day), $A = K_2HPO_4{\cdot}3H_2O$ (g/L), B = citric acid (g/L), and C = trace metal solution (mL/L).

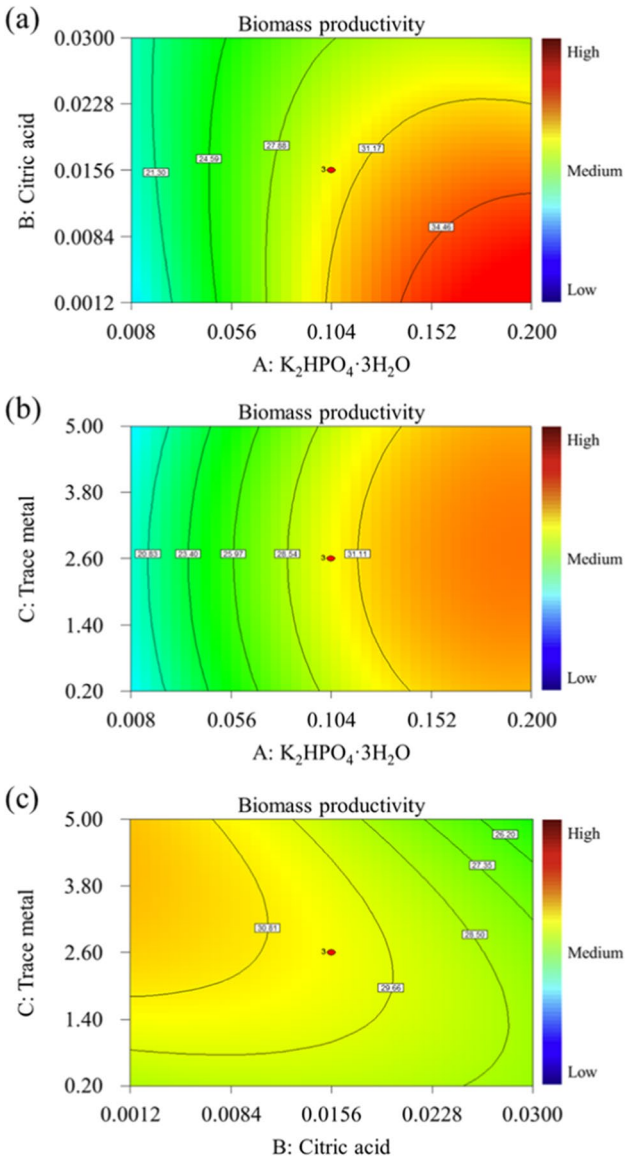

Fig. 1 2D Contour plots showing the effect of **a** $K_2HPO_4{\cdot}3H_2O$ (g/L), **b** Citric acid (g/L) and **c** trace metal (mL/L) on biomass productivity (mg/L/day). One variable kept constant at its center point and other two variables varied within the experimental range

The *F*-test and ANOVA were used to validate Eq. (21) for the model, and the results are shown in Table 4. The *P*-value of the model was 0.01, suggesting the model was highly significant at the 99% confidence level and the biomass productivity can be well-explained by this model. The model *F*-value of 8.36 implies that the quadratic model for the biomass productivity was significant. According to Pandey and Kumar [36], a significant model is one with a high *F*-value but a low *P*-value. Interestingly, the *P*-value of lack of fit indicates a suitable score (*P*-value > 0.05), indicating that the residual error to the pure error from the replicated experimental design points showed an insignificant difference [24]. The low pure error value (2.65) also indicated good reproducibility of the data. The multiple correlation coefficient or R^2 of the regression equation was 0.91, indicating that up to 91% of the variations in response can be explained by the model. The low coefficient values (13.74%) demonstrated that the experiments were highly accurate and reliable. Similarly, Srinuanpan et al. [27] reported that a suitable CV value of the model should be lower than 20%.

Through ANOVA (Table 4), the linear term of $K_2HPO_4{\cdot}3H_2O$ (*A*) and quadratic terms of $K_2HPO_4{\cdot}3H_2O$ (A^2) significantly influenced the biomass productivity with *P*-values less than 0.05, demonstrating that the enhancement of the biomass productivity required a suitable $K_2HPO_4{\cdot}3H_2O$ concentration. Contour plots based on Eq. (21) with one variable kept constant at its center point and the other two variables varied in their ranges are shown in Fig. 1. These figures were plotted to analyze the interactions among independent variables and to identify the best level for the intended response of each variable. Figure 1a presented the effects of $K_2HPO_4{\cdot}3H_2O$ and citric acid on the biomass productivity at a trace metal solution of 2.6 mL/L. The biomass productivity increased with increasing $K_2HPO_4{\cdot}3H_2O$ concentration and decreasing citric acid concentration. According to Lv et al. [37], the increased $K_2HPO_4{\cdot}3H_2O$ concentration (0.02–0.10 g/L) is expected to provide a rapid growth rate of *Nostoc flagelliforme* and therefore higher biomass productivity. This was due to the fact that the phosphorus and potassium in $K_2HPO_4{\cdot}3H_2O$ are both required nutrients for cyanobacterial growth. However, further addition of $K_2HPO_4{\cdot}3H_2O$ (> 0.08 g/L) resulted in decreased biomass productivity owing to substrate inhibition [30]. In addition, a high concentration of added acids such as citric acid and lactic acid may change the pH to an unfavorable range, affecting the biomass productivity [38]. Figure 1b showed the interaction effect between $K_2HPO_4{\cdot}3H_2O$ and trace metal solution on the biomass productivity. When citric acid was set at the center point of 0.0156 g/L, the maximum biomass productivity was obtained when using the highest $K_2HPO_4{\cdot}3H_2O$ concentration tested, and a moderate concentration of tested trace metal solution. Facey et al. [5] and de Oliveira et al. [39] reported that cyanobacteria and microalgae are required in very low concentrations of trace metal solution that are still necessary for cell growth. Low concentrations promote the healthy growth of microalgae and cyanobacteria, while large concentrations have harmful effects. Figure 1c depicted the interaction effect between citric acid and trace metal solution on biomass productivity; it was observed that low citric acid and moderate trace metal solution did improve the biomass productivity. A similar observation was reported by Facey et al. [5], Kim et al. [38], and de Oliveira et al. [39].

Overall, the importance of the degree of the three nutrient components on the biomass productivity of *Nostoc* sp. AARL C008 biomass in this study would be as

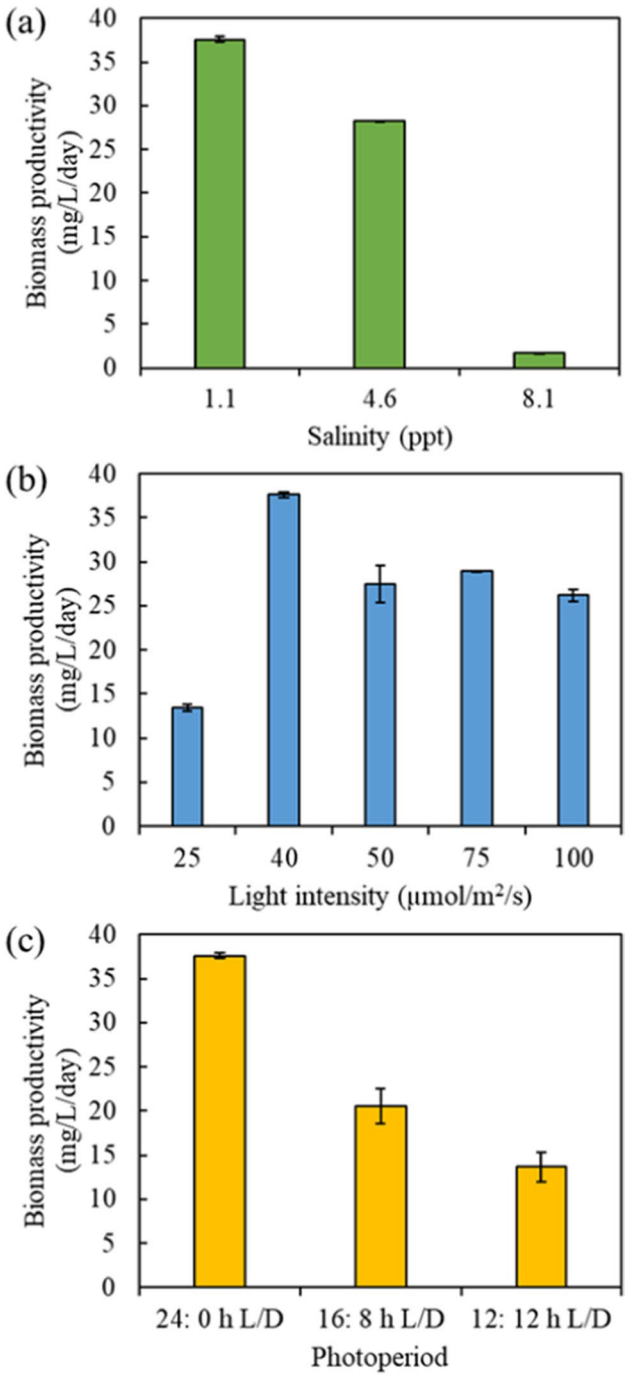

Fig. 2 Effect of salinity, light intensity, and photoperiod on biomass productivity of cyanobacterial *Nostoc* sp. AARL C008

follows: $K_2HPO_4{\cdot}3H_2O$ > citric acid > trace metal solution, and for the interaction effects it would be as follows: $K_2HPO_4{\cdot}3H_2O$ vs. citric acid > citric acid vs. trace metal solution > $K_2HPO_4{\cdot}3H_2O$ vs. trace metal solution. The optimum conditions for maximizing biomass productivity of cyanobacterium *Nostoc* sp. AARL C008, calculated by setting the partial derivatives of Eq. (21) to zero with respect to the corresponding variables, were a $K_2HPO_4{\cdot}3H_2O$ concentration of 0.190 g/L, a citric acid concentration of 0.0018 g/L, and a trace metal solution of 2.53 mL/L. The maximum response value for the biomass productivity was estimated to be 37.25 mg/L/day. Three replicates of the experiments were performed under the optimal conditions, which would give the biomass productivity as high as 37.59 ± 0.34 mg/L/day. The experimental values were very similar to the predicted values without significant difference ($P < 0.05$).

3.1.2 Optimization of physicochemical factors

Effect of salinity The effects of different salinities on the biomass productivity of cyanobacterium *Nostoc* sp. AARL C008 grown in optimized BG-11 medium with and without NaCl supplementation are shown in Fig. 2a. The results found that at 4.6 and 8.1 ppt the biomass productivity was decreased by up to 24.87% and 95.42%, respectively, when compared with the control (salinity of 1.1 ppt), while with a high salinity at > 8.1 ppt the cyanobacteria did not grow, indicating that the biomass productivity of *Nostoc* sp. AARL C008 decreased sharply with increasing salinity. As these cyanobacteria originated from freshwater, the excessive quantity of salt probably hindered growth and metabolism. Silveira and Odebrecht [6] have reported that the reduction in cyanobacteria growth may be attributed to the reduced photosynthesis with salt addition. Salinity stress also impacts cyanobacteria through the osmotic pressure and ion homeostasis mechanisms, changing ionic ratios in the cells owing to the membrane's selective ion permeability [40]. This is incongruous with another study in salt tolerant *Dunaliella salina* and *Chlorella vulgaris* which showed that both algae could grow at a high salinity of 32–197 ppt [41, 42]. However, increasing the salt dosage is costly. Thus, based on this study, the optimized BG11 medium without NaCl supplementation could be used as an effective medium for maximizing the biomass productivity of *Nostoc* sp. AARL C008.

Effect of light intensity Concerning the light intensity study, the effects of light intensity on the biomass productivity of cyanobacterium *Nostoc* sp. AARL C008 are shown in Fig. 2b. The results revealed that increasing the light intensity from 25 to 40 µmol/m^2/s improved biomass production and reached the maximum biomass productivity of 37.59 mg/L/day. An additional increase in light intensity did not enhance biomass production. The results correspond to general fundings, which show that light intensity over a certain taxa-dependent saturation threshold limits the cell growth of cyanobacteria and microalgae, and indicate that further increases would lead to photoinhibition [7, 43]. At light intensities lower than the optimal level, photolimitation occurred and resulted in lower biomass productivity [44]. It

was reported by de Oliveira et al. [45] that *Nostoc* sp. F105 grew better at a light intensity of 40 µmol/m^2/s. For *Nostoc calcicola*, the optimal light intensity was lower at 21 µmol/m^2/s [7]. Ma et al. [8] reported that *Nostoc sphaeroides* grew well when the light intensity was increased up to 90 µmol/m^2/s. Different cyanobacteria species respond differently to light intensity. It could be concluded that the optimum light intensity for *Nostoc* sp. AARL C008 is 40 µmol/m^2/s.

Effect of photoperiod Lastly, as far as the parameter of the photoperiod is concerned, the effect of photoperiod was investigated using the optimal BG11 medium without salt supplementation and the optimal light intensity of 40 µmol/m^2/s (Fig. 2c). It was observed that *Nostoc* sp. AARL C008 grew best at light:dark cycles of 24:0 h and gave the maximum biomass productivity of 37.59 mg/L/day. The biomass productivity was significantly decreased by 45–64% when the photoperiod was decreased from 24 to 12 h. This could be due to a shortage in light energy supply. A light period of 12–16 h is insufficient to store enough energy to sustain cell development during an 8–12 h non-light phase. Similar observations have been reported by Thawechai et al. [46] and Sirisuk et al. [47]. It has been reported that moderate light intensity coupled with a long photoperiod might lead to the enhancement of *Nostoc* growth and later biomass productivity [9]. It should be noted that continuous light feeding generates remarkably greater biomass productivity, indicating that biomass production of cyanobacteria might be photo-dependent and that light is necessary for the process. Therefore, the optimum photoperiod for *Nostoc* sp. AARL C008 is light:dark cycles of 24:0 h.

Following several optimization stages employed in this study, these indicated that high-throughput bioprocess optimization of growth medium and key physicochemical factors were effective approaches to maximize the biomass productivity of *Nostoc* sp. AARL C008. Compared to before optimization (25.58 mg/L/day), the biomass productivity after optimization significantly increased by 1.47 folds. However, the biomass productivity in this study was lower than that in the report of Lee et al. [48] (0.32–0.42 g/L/day). This might be due to different culture conditions used, environmental adaptation ability, and algal isolation source. Thus, further research and development are still required since the optimum growth varies depending on the strain cultivated and operating conditions used.

3.2 Application in multiproduct biorefinery

Three economically important fractions including polysaccharides, phytochemicals, and lipids were sequentially recovered from the cyanobacterial biomass of *Nostoc* sp. AARL C008 using an integrated biorefining process. The zero-waste biorefining process for multi-production is composed of three main steps: (I) polysaccharide extraction for preparing biostimulants, (II) phytochemical extraction from polysaccharide-free residual powdered biomass (PRPB) for preparing antioxidative and anticancer phytochemicals, and (III) lipid extraction from polysaccharide–free and phytochemical-free residual powdered biomass (PPRPB) prior to transesterification to produce biodiesel.

3.2.1 Biostimulant activity of polysaccharide extract

Polysaccharides from cyanobacterium *Nostoc* sp. AARL C008 were extracted using hot water and then partially purified by alcohol precipitation (resulting in crude polysaccharide extract: CPS). Both hot water extraction and alcohol precipitation are established and very efficient methods that are widely employed for the extraction and purification of polysaccharides, even on a large scale in industrial contexts [13]. The extraction yields of CPS were 48.61 g/kg-biomass and CPS had the total sugar content and total reducing sugar content at 46.73 and 27.92% w/w, respectively. Generally, cyanobacterial *Nostoc* spp. develops macroscopic colonies, with filaments embedded in extracellular polysaccharides (EPS), which serve as a support for the colony [49], indicating that the water-soluble CPS in this study is mainly EPS. Similar results were also found by Tiche et al. [17], while Wang et al. [49] reported that water-soluble polysaccharides from *Nostoc* sp. and *Nostoc commune* yielded in a range of 4–10% w/w with a total sugar content of 9–18% w/w and reducing sugar content of 6–11% w/w.

The monosaccharide compositions of CPS had the highest content of mannose at 136.80 mg/g CPS, followed by glucose (109.68 mg/g CPS) and xylose (93.36 mg/g CPS), respectively, while rhamnose, psicose, fructose, allose, mannose, and sucrose were not observed in CPS (Table S1, See supplementary data). In the literature, Li et al. [50] found that the monosaccharides in the water-soluble polysaccharide extracted from *Nostoc sphaeroides* were 34.5% mannose, 21.8% fructose, 14.6% galactose, 17.7% glucose, 6.1% xylose, 2.2% rhamnose, and 3.1% galacturonic acid, while the report of Shen et al. [51] highlighted that the monosaccharide composition in CPS extracted from *Nostoc flagelliform* was mainly composed of mannose (19.80%), galactose (23.71%), glucose (46.57%), and glucuronic acid (4.00%). Furthermore, they contained trace amounts of xylose, arabinose, ribose, rhamnose, fucose, and fructose. They are different depending on strains and the extraction methods and conditions [57]. As previously discovered by methylation and gas chromatography–mass spectrometry analysis, xylose and glucose were 1 → 4 linked; mannose and xylose were terminal groups; and branch points occurred in glucose as 1 → 3,4 and 1 → 3, 6 linkages and in xylose as a 1 → 3, 4 linkage [50].

The FTIR spectrum for CPS is shown in Fig. S1 (See supplementary data). A peak at 3276 cm^{--1} indicated the

presence of asymmetric OH-stretching, suggesting the presence of intra- and intermolecular hydrogen bonds [52]. The absorption peaks at 2973 cm^{-1} and 1200 to 1400 cm^{-1} correspond to the stretching and angular vibration of a C–H bond, indicating CPS is a carbohydrate [53]. The moderate-strength absorption peak around 1641 cm^{-1} was from C = O stretching vibration, suggesting that CPS may contain acetyl or uronic acid groups. The absorption peak at 1408 cm^{-1} likely relates to C – H bending vibration, while the band at 1243 cm^{-1} can be assigned to the stretching of an S = O bond. The strong absorption peak at 1026 cm^{-1} is from C – O stretching in a primary alcohol OH, which is the characteristic absorption peak of the pyranose carbohydrate ring [52]. In addition, the band at 806 cm^{-1} was consistent with the presence of α-type glycosidic linkages between glycosyl residues, and the peaks at 563 cm^{-1} were due to C – H rocking vibration. Previously, similar peaks were also reported for the FTIR spectrum of a polysaccharide extracted from *Nostoc sphaeroides* [50, 54]. Collectively, the FTIR spectrum of CPS exhibited the typical absorption bands that are indicative of polysaccharides.

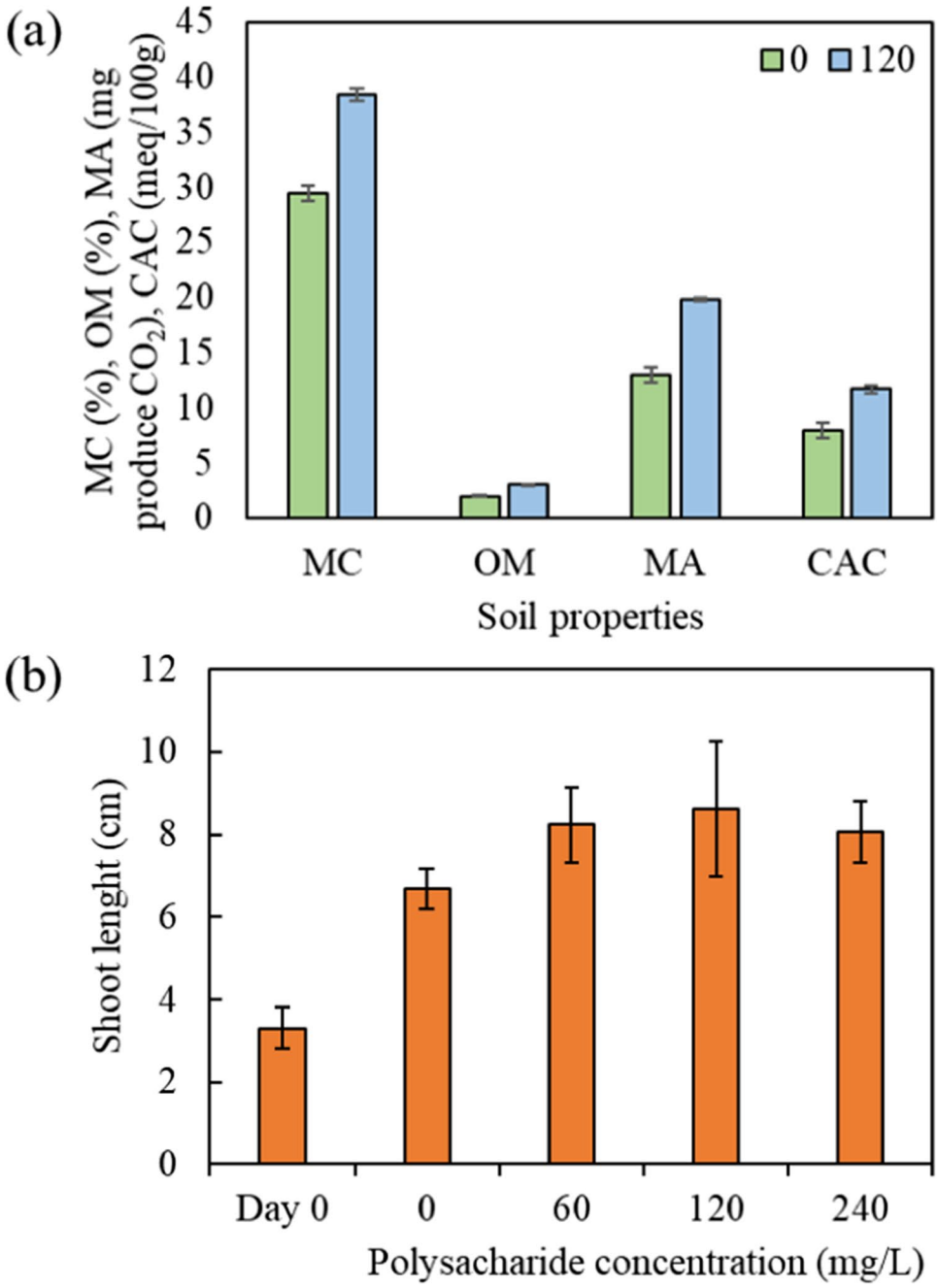

Fig. 3 Effect of *Nostoc* polysaccharide on soil properties (moisture content (MC), organic matter (OM), microbiological activity (MA), and cation exchange capacity (CEC)) after 15 days of inoculation at 0 and 120 mg/L polysaccharide (**a**) and shoot length of melon after 4 weeks of cultivation at 0, 60, 120, and 240 mg/L polysaccharides (**b**)

CPS was further characterized by NMR analysis. The ^{1}H-NMR spectrum is shown in Fig. S2. The spectra showed ring protons (3.2–4.2 ppm), indicating a crowded signal region due to the presence of many sugar residues; this region is typical for polysaccharides; and a signal at 2.25 ppm, indicating that the polysaccharide contains acetyl groups. Methyl protons (1—1.3 ppm) were also observed in the ^{1}H-NMR spectrum. Similar regions have been reported in microalgae and cyanobacteria 1H-NMR spectra [52, 55]. However, the appearance of several overlapping signals in the ^{1}H-NMR spectra was an indicator that was difficult to decipher because of its complexity, indicating that CPS were very complex polysaccharides, in agreement with previous reports [56]. Thus, further studies are required to fully characterize the CPS to expand the current understanding of the complicated occurrences in the CPS structure.

Considering the soil improvement ability of CPS (Fig. 3a), it was found that the moisture content (38.40%), organic matter (3.07%), microbiological activity (19.84 mg produced CO_2), and cation exchange capacity (11.67 meq/100 g) of soil after 15 days of CPS inoculation were significantly increased 1.30, 1.55, 1.53, and 1.47-fold, respectively, compared to the control as deionized water-inoculated soil. The enhancement of soil moisture may be related to the fact that cyanobacterial polysaccharide sheaths have the capacity to absorb significant quantities of water, which results in a substantial increase in soil water absorption and retention [58]. Chamizo et al. [59] suggested that increased water availability stimulates microbiological activity, resulting in higher organic matter, and nutrient content. Most plants grow within soil moisture levels that vary between 20 and 60% [60]. A significant increase in the nutritional content and cation exchange capacity of soils is attributed to the action of the polysaccharide as a nutrient repository, sequestering metabolites produced by microorganisms, in particular amino acids and organic acids, as well as metal cations such as Ca^{2+} and Mg^{2+} [59]. Therefore, this study highlighted that the inoculation of soil with *Nostoc* CPS may possibly be utilized as a sustainable biotechnological method to restore damaged dryland sites because of the significant environmental function performed by *Nostoc* CPS.

In addition to the soil improvement ability, the plant growth promotion potential of CPS was also evaluated using green net melon as a plant model. After 4 weeks of cultivation, the CPS addition at 60, 120, and 240 mg/L significantly increased the shoot length of the melons 1.23, 1.29, and 1.20-fold, respectively, which was greater than the control which featured the absence of CPS (Fig. 3b). This observed growth enhancement in melons may be due to the presence of CPS extracted from *Nostoc* sp. AARL C008. As a result of these findings, it is possible to argue that cyanobacterial polysaccharides may be used as a source of plant biostimulants for crop development. In addition, the enchantment of melon might be due to the improvement in soil properties by CPS and the release of nutrients required by plants [59]. Similar results have also been observed in the report of Rachidi et al. [61] and Santini et al. [62]. Rachidi et al. [61] suggested that the presence of monosaccharide (glucose, xylose, and mannose) may have been the primary polysaccharide components at the time of the onset of biostimulation. It seems that inoculation with cyanobacterial polysaccharides has an impact on many metabolic pathways in plants, including photosynthesis and nitrate assimilation, resulting in the enhancement of plant growth, according to the results of Saucedo et al. [63]. According to Fig. 3b, it was also observed that the shoot length of melons increased when increasing the CPS concentration, but decreased at high CPS concentrations above 240 mg/L. A decrease in plant growth with increasing cyanobacterial polysaccharide concentration was also reported by Tiche et al. [17] and Xu et al. [64]. This phenomenon might be due to the excessive polysaccharide levels entering the plant cells. Xu et al. [64] reported that an excess of polysaccharide resulted in the overproduction of reactive oxygen species (ROS), which are harmful to the normal metabolism of plant cells and cause oxidative damage to photosynthetic systems through the induction of lipid peroxidation, protein degradation, and DNA damage, resulting in a decrease in the plant growth rate. Therefore, the suitable concentration of *Nostoc* CPS for growth promotion of melon was 120 mg/L.

3.2.2 Bioactivities of phytochemical extract

Phytochemicals from polysaccharide-free residual powdered biomass (PRPB) were extracted using mixed solvent extraction (ethyl acetate–methanol, 1:1 v/v). According to Wakeel et al. [65], the combination of solvent was the most efficient solvent in terms of phytochemical quantity and quality. It has been reported that ethyl acetate–methanol proved to be the significant solvent of choice to maximize phytochemical content and provide essential biological properties [65, 66]. The results found that the extraction yield of *Nostoc* phytochemicals from PRPB was 21.97 g/kg-PRPB (20.9 g/kg-biomass) which was in line with previously reported extraction yields (0.1–10% w/w) obtained from different *Nostoc* biomass, and many factors have contributed to the phytochemical yield [67, 68]. The phytochemical extract contained chlorophyll a, carotenoids, and phenolics at 38.16 mg/g extract, 279.43 mg/g extract, and 11.43 mg GAE/g extract, respectively. Considering phytochemical absorption patterns via the UV/visible spectrum (250–750 nm) (Fig. 4a), three main absorption peaks were found at 250–315 nm, 320–550 nm, and 600–710 nm. These findings have been confirmed by previous observations showing phytochemical extracts comprise many components, such as pigments that absorb UV–visible light [69]. Interestingly, phytochemical extracts showed peaks at 250–280 nm (UV-C), 280–315 nm

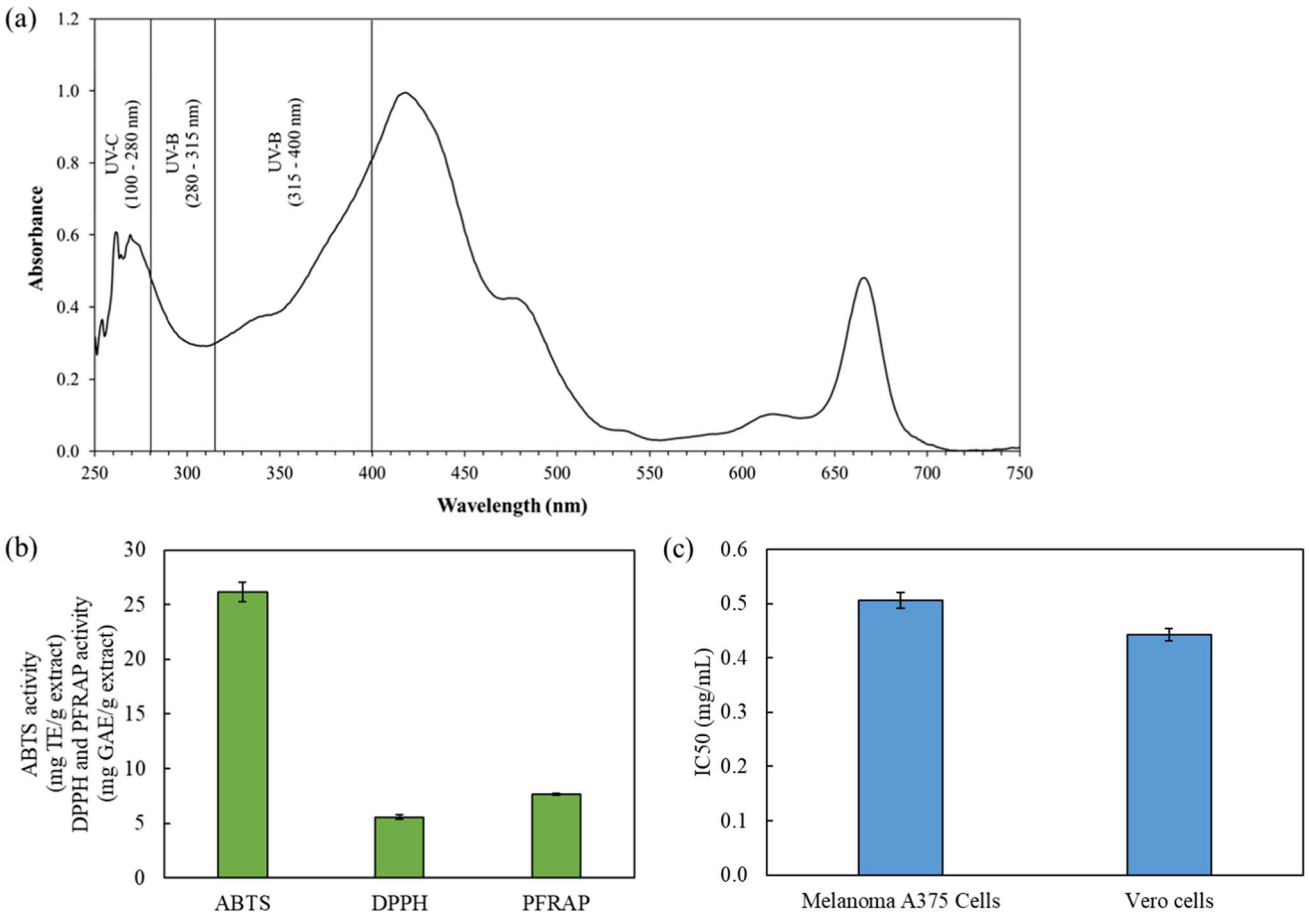

Fig. 4 UV–Vis absorption spectra (**a**), antioxidant activities (**b**) and anticancer properties (**c**) of EtOAc/MeOH extract from cyanobacterial *Nostoc* sp. AARL C008 biomass

(UV-B), and 315–400 nm (UV-A), indicating that the extract could be considered in the formulation of a sunscreen to protect the skin by reducing UV ray penetration and UV ray damage. Cyanobacterial pigments such as chlorophylls and carotenoids absorb light at wavelengths of 400–500 nm and 600–700 nm [70]. The extract showed a peak between 266 and 374 nm which corresponds to phenolic compounds such as flavonoids, flavonols, and anthraquinones [71]. It should be noted that UV/visible absorbance varies according to the chemicals present in the phytochemical extract. Similar observations were also documented by different authors for *Nostoc* sp. and other cyanobacteria [67, 68]. Further studies on the full characterization of the extracts are required to expand the current understanding of the complicated UV/vis absorption patterns of phytochemical extracts.

The antioxidant activity of *Nostoc* phytochemical extract was evaluated including ABTS radical scavenging activity, DPPH radical scavenging activity, and potassium ferricyanide reducing antioxidant power (PFRAP) activity. As shown in Fig. 4b, the ABTS and DPPH radical scavenging activity of the phytochemical extract were 26.10 mg TE/g extract and 5.71 mg GAE/g extract, respectively, indicating that *Nostoc* phytochemical possibly contains effective hydrogen-donating compounds that will neutralize the ABTS and DPPH free radicals to a more stable form. *Nostoc* phytochemicals could possibly be utilized as an oxidation inhibitor by scavenging ABTS and DPPH free radicals or other related free radicals to protect cells from oxidative stress. These results are comparable with the antioxidant values of phytochemicals obtained from different cyanobacteria reported by Ijaz and Hasnain [72] and Vega et al. [73]. The PFRAP activity was also measured to evaluate the ability of phytochemical extract in reducing Fe^{3+} to Fe^{2+}. The results found that *Nostoc* phytochemicals recorded PFRAP activity at 7.79 mg GAE/g extract (Fig. 4b) which was in good agreement with the previous study reported by Yasin et al. [74]. This proved that *Nostoc* phytochemicals serve as high-efficiency reductants by giving an electron to free radicals, stabilizing them, and reducing free radical-induced cell and DNA damage [24].

Figure 4c shows the in vitro antiproliferative activity on malignant melanoma cells (A375 skin cancer cells)

and normal cells (Vero cells). The results found that *Nostoc* phytochemicals exhibited antiproliferative activity on A375 skin cancer cells with the IC_{50} of 0.50 mg/mL and Vero cells with the IC_{50} of 0.44 mg/mL, which are aligned with Karan and Aydin [75]. Although the extract had excellent antiproliferative activity against A375 skin cancer cells, the greater Vero cells' sensitivity in comparison with cancer cells might harm normal human cell proliferation. According to Ruangrit et al. [13] and Umthong et al. [26], the addition of an extract purification step resulted in the greatest inhibition on cancer cell lines, but the least inhibition on normal cells. Thus, *Nostoc* phytochemical extract should be further purified and examined to measure its potential biological function before acting as the template for future drug design. In the literature, the presence of chlorophylls, carotenoids, and phenolics in the extract can be correlated with their antioxidant and anticancer activities [72–75]. This indicated that detected chlorophylls, carotenoids, and phenolics were responsible for the antioxidant and anticancer activities of *Nostoc* phytochemical extract in this study, and *Nostoc* phytochemical extract could be considered to be a potential bioactive ingredient for use in the nutraceutical, cosmetic, and pharmaceutical industries. However, these still contained various unidentified compounds that can contribute to antioxidant and anticancer activities. Therefore, further research is required to gain an understanding of the complete profile of the phytochemical extract, which will help to support the overview of bioactive compounds found in the extract.

3.2.3 Biodiesel production

The polysaccharide-free and phytochemical-free residual powdered biomass (PPRPB) was used to extract the cyanobacterial lipids which were then acid-transesterified to fatty acid methyl esters (FAMEs). The lipid content was 102.10 g/kg PPRPB (95.00 g/kg biomass). This result was similar to the findings of de Oliveira et al. [76], who reported that the lipid content measured in three cyanobacteria including *Cyanobium* sp., *Limnothrix* sp., and *Nostoc* sp. ranged from 0.4 to 10% w/w. Fatty acid (FAs) profiles of PPRPB lipid are summarized in Table 5. A variety of C6 to C24 fatty acid chain lengths has been accumulated in the *Nostoc* lipid. Long-chain fatty acids with 16 and 18 carbon atoms (> 96%) were the most predominant fatty acids including palmitic acid (C16:0; 46.49%), palmitoleic acid (C16:1; 18.69%), oleic acid (C18:1n9c; 13.10%), elaidic acid (C18:1n9t; 6.89%), linoleic acid (C18:2n6c; 6.61%), and stearic acid (C18:0; 3.24%). These fatty acids are comparable to those found in plant oils, which are mostly composed of palmitic acid and oleic acid [77], so it is reasonable to conclude that cyanobacterial lipids hold promise as biodiesel feedstocks. The European biodiesel standard specifies that the maximum levels of fatty acids, with more than four double bonds, should not exceed 1%, whereas linoleic acid (C18:3) should be less than 12%. Both criteria were satisfied in this study as the identified fatty acids include only a small quantity of polyunsaturated fatty acids (those with four or more double bonds) at < 0.1% while C16:3 fatty acid was found at only 0.91% (Table 5). Lipids having long-chain fatty acids

Table 5 Fatty acid profiling of cyanobacterial lipid extracted from polysaccharide-free and phytochemical-free residual powdered biomass (PPRPB) of *Nostoc* sp. AARL C008

Fatty acids	Relative content (%)
C6:0	0.01
C8:0	0.02
C10:0	0.04
C11:0	0.02
C12:0	0.11
C13:0	0.04
C14:0	0.72
C14:1	0.12
C15:0	0.44
C15:1	0.08
C16:0	46.49
C16:1	18.69
C17:0	0.54
C17:1	0.32
C18:0	3.24
C18:1n9c	13.10
C18:1n9t	6.89
C18:2n6c	6.61
C18:3n6	0.91
C20:0	0.07
C20:1n9	0.49
C20:2n6	0.07
C20:4n6	0.17
C20:5n3	0.02
C21:0	0.01
C22:0	0.09
C22:1n9	0.63
C23:0	0.01
C24:0	0.04
C24:1n9	0.01
C16-C18	96.78
SFA	51.87
UFA	48.13
MUFA	40.34
PUFA	7.78
SFA/UFA	1.08

SFA saturated fatty acid, *UFA* unsaturated fatty acid, *MUFA* monounsaturated fatty acid, *PUFA* polyunsaturated fatty acid

Table 6 Estimated fuel properties of *Nostoc* lipid extracted from polysaccharide-free and phytochemical-free residual powdered biomass (PPRPB)

Parameters	Values	ASTM D6750	European (EN-14214)
Saponification value (SV, mg KOH/g oil)	201.46	< 202	–
Iodine value (IV, g I_2/100 g oil)	50.63	–	≤ 120
Cetane number (CN)	62.00	> 47	> 51
Degree of unsaturation (DU, %wt)	55.90	–	–
Long-chain saturated factor (LCSF, %wt)	6.56	–	–
Cold filter plugging point (CFPP, °C)	4.13	–	< 5– < − 20
Cloud point (CP, °C)	19.46	3	> 4
High heating value (HHV, MJ/kg)	40.41	–	–
Kinematic viscosity (υ, ln KV at 40 °C in mm^2/s)	5.63	1.9–6.0	3.5–5.0
Density (ρ, g/cm^3)	1.14	0.85–0.90	0.86–0.90
Oxidative stability (OS; h)	18.28	> 3	> 6
Allylic position equivalents (APE)	55.03	–	–
Bis-allylic position equivalents (BAPE)	8.42	–	–

(> 90% of C16–C18 fatty acids), as proposed by Cheirsilp et al. [78], have the potential to be utilized as an effective feedstock for biodiesel production. More than 92% of the *Nostoc* lipid examined in this study included saturated fatty acids (SFA) and monounsaturated fatty acids (MUFA). This seems to mean that using the *Nostoc* lipid as a substrate for biodiesel production will lead to environmentally friendly biodiesel with a higher cetane number, reduced NOx emissions, shorter ignition delay time, and better oxidative stability. Similar findings were reported by Srinuanpan et al. [27], who discovered that a greater concentration of SFA and MUFA plays a significant role in the production of biodiesel with improved fuel characteristics. Moreover, this study found that *Nostoc* lipid extracted from PPRPB had an SFA/UFA ratio of 1.08. Ruangrit et al. [13] and Srinuanpan et al. [44] suggested that an increased SFA/UFA ratio gives better density and viscosity values, and the biodiesel produced has stronger oxidative stability.

The characteristics of biodiesel produced from *Nostoc* lipid were estimated based on their fatty acid methyl ester (FAMEs) profiles, and the results are presented in Table 6. The saponification value (SV) of *Nostoc* biodiesel was found to be 201.46 mg KOH/g oil, which corresponds to the quantity of KOH (in milligrams) required for the saponification of 1 g of oil. These values are comparable to those previously observed in cyanobacteria [79]. In the ASTM biodiesel standard for biodiesel, the highest allowable SV value was 202 mg KOH/ g oil [80]. The iodine value (IV) of *Nostoc* biodiesel was 50.63 g I_2/100 g oil, which is in compliance with the European biodiesel standard (EN-14214) (< 120 g I_2/100 g oil). Normally, IV is an indication of the total unsaturation of biodiesel and is used to indicate the oxidative stability of the fuel. A low IV suggested a greater degree of oxidative stability [27]. This demonstrates the *Nostoc* biodiesel's resistance to oxidation. The cetane number (CN) of *Nostoc* biodiesel reached as high as 62, guaranteeing higher ignition quality, while the international regulations (ASTM and EN-14214) specify a minimum limit of 47 for CN. The degree of unsaturation (DU) of *Nostoc* biodiesel was 55.9% which is almost equal to cyanobacteria *Synechocystis* sp. (61.9%) [79]. Ruangrit et al. [13] suggested that a lower DU value indicates that the biodiesel is more oxidatively stable when stored for an extended period of time. The biodiesel flow behavior consisting of long-chain saturated factor (LCSF) and cold filter plugging point (CFPP) were 6.56% and 4.13 °C, respectively, showing insufficient quality in tropical countries while being easy to use in cold regions. Similar results were documented by Karpagam et al. [81]. A vehicle's cloud point (CP) is defined as the temperature at which the fuel begins to look hazy and verifies the development of wax crystals in the fuel, which clogs the vehicle's filters and fuel lines. Despite the fact that the international biodiesel standard does not include a minimum temperature in its list of requirements, a lower range of CP is more appropriate according to the report of Sivaramakrishnan and Incharoensakdi [82]. The CP (19.46 °C) found in this study increases the acceptability of biodiesel for use at low temperatures. The higher heating value (HHV) of biodiesel is the unit amount of fuel that produces heat after it has been completely burned. The HHV of *Nostoc* biodiesel was as high as 40.41 MJ/kg which is almost equal to petroleum-derived diesel (46 MJ/kg) [82].

According to Table 6, it was also observed that the kinematic viscosity (υ) of *Nostoc* biodiesel was 5.63 which corresponded to the international biodiesel standard for υ with 1.9–6.0. The υ of fluid is a measure of how resistant it is to flowing. The quality of the fuel increases when the viscosity of the fuel is reduced, since the spray properties of the fuel

are greatly affected by the viscosity and density of the fuel. Sharma et al. [83] found that the increased viscosity causes a low fuel spray on CI engines, leading to incomplete combustion and carbon buildup on the injector and valve sheet, which may cause severe engine issues. Density (ρ) also influences the spray properties of fuel in CI/SI engines and has a direct impact on the combustion behavior. The ρ of *Nostoc* biodiesel (1.14 g/cm^3) in this study was found to be higher than the international biodiesel standard (0.85–0.90). This might be owing to the existence of unsaturated FAMEs in biodiesel [2, 83]. One of the most serious issues regarding biodiesel's poor qualities is its oxidation stability (OS). An increase in polyunsaturated fatty acid levels in the FAMEs results in a reduction in the OS [82]. In this study, the OS of *Nostoc* biodiesel was as high as > 18 h which was found to be higher than the international biodiesel standard, revealing good oxidation stability. The allylic position equivalent (APE) and bis-allylic position equivalent (BAPE) are indices that are used to correlate the structure and quantity of alkyl esters contained in biodiesel with the oxidative stability of that fuel. The APE and BAPE of *Nostoc* biodiesel in this study were 55.03 and 8.42, respectively. Dwivedi and Sharma [84] and Verma et al. [85] reported that the APE and BAPE of various vegetable oil feedstocks were in the range of 17–189 and 4–85, respectively. They also suggested that the oil with the lowest BAPE content be utilized for biodiesel synthesis, noting the oil's excellent oxidation stability. In addition, oxidation stability can be measured by the oxidation stability index (OSI) which is corelated to both APE and BAPE [84]. Verma et al. [85] found that an increase in BAPE leads to a decrease in OSI, indicating that oils worsen in oxidation stability parameters. The OSI of *Nostoc* biodiesel in this study was 3.53 h which was in good agreement with the previous study reported by Dwivedi and Sharma [84] and Verma et al. [85] who revealed that the OSI values of various vegetable feedstocks were recorded in the range of 0.1–3.7 h. They also suggested that oils with a higher OSI offer promising possibilities as prospective feedstocks due to their excellent oxidation stability properties. Therefore, since both ASTM D6751 (USA) and EN 14,214 (European Organization) standards refer to biodiesel, it is feasible to state that the fuel characteristics of *Nostoc* lipid meet these requirements, which implies they are appropriate for biodiesel feedstock.

3.2.4 Proposed biorefinery approach of cyanobacterial biomass

A sustainable biorefining approach has now been employed to maximize the utilization of cyanobacterial biomass for the integrated production of further valuable biochemicals with a demonstrated market value [2]. Biorefining is clearly advantageous because the sequential concentration of residual biomass requires fewer reactants than an individual extraction of the biochemical component in consecutive extraction stages [13, 86]. Hence, we propose a bioprocessing route for the establishment of an integrated biorefinery based on cyanobacterium *Nostoc* sp. AARL

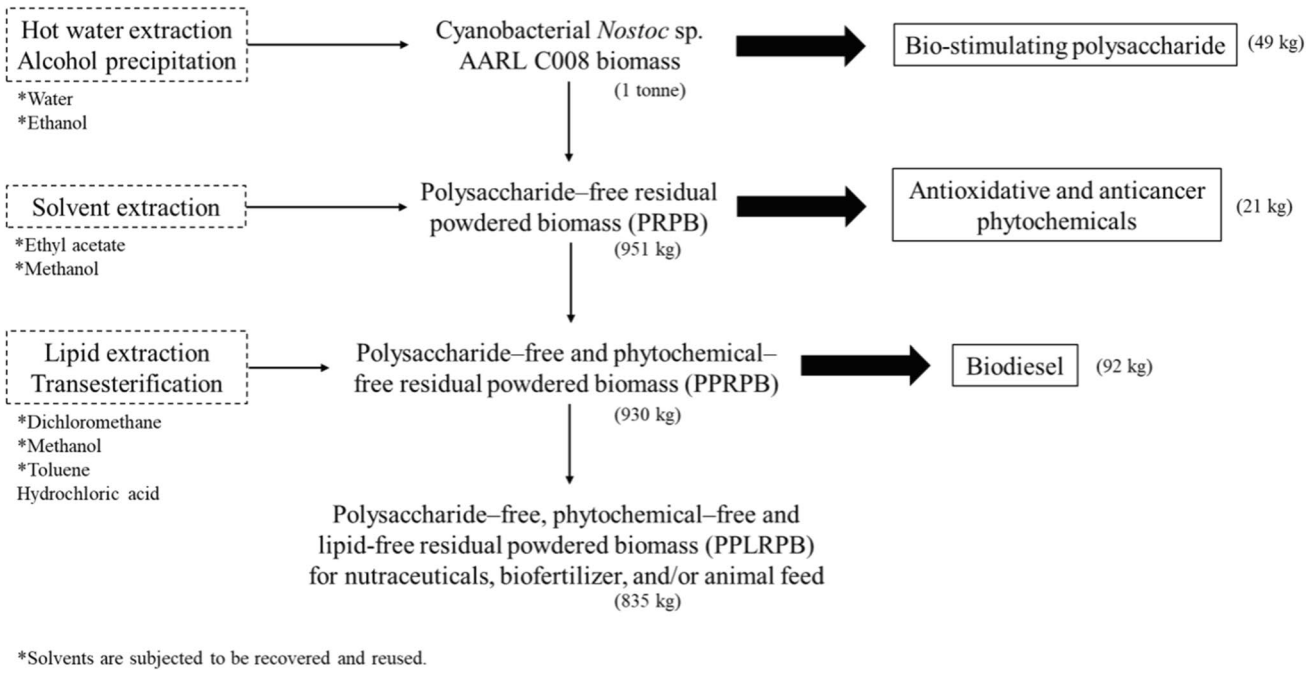

Fig. 5 A proposed scheme to establishing a multiproduct cascading zero-waste biorefinery process for cyanobacterial biomass

C008 biomass (Fig. 5). It is evident from the computation of data that one ton of *Nostoc* biomass could give approximately 49 kg of bio-stimulating polysaccharide, 21 kg of antioxidative and anticancer phytochemicals, and 95 kg of lipid on a dry weight basis. Further, 95 kg of lipid produced 92 kg of biodiesel, which was computed using literature conversion factors [87]. The solvents employed in the process are prone to be readily recovered and reused, which decreases the demand for reagents and, as a consequence, lowers the total production cost of the process. After the biorefinery process, the residual biomass was recovered which could be used as promising feedstock for cosmetic and nutraceutical protein hydrolysates [24], environment-friendly biofertilizer [88], and economical animal feed [1]. Nonetheless, further research and analysis are required in order to make the best decision. It should be emphasized that the biorefinery process proposed in this study has the potential to reduce the cost of producing value-added products from cyanobacterial biomass without producing waste and also allows for the full realization of the potential provided by biomass resources. Therefore, our findings indicate a significant improvement in biomass processing technology toward the sustainable development of cyanobacteria-based industries.

4 Conclusions

This study showed that high-throughput bioprocess optimizations using Plackett–Burman design (PBD) and central composite design (CCD) were effective approaches to screen and optimize the growth medium of the cyanobacterium *Nostoc* sp. AARL C008. Key physicochemical factors were optimized to obtain maximum biomass productivity. Cyanobacterial *Nostoc* biomass can be employed as a promising environmentally friendly and sustainable feedstock for multiproduct application through effective zero-waste biorefining processes which could significantly improve the completeness of the cyanobacteria-based industries. *Nostoc* polysaccharide recovered by hot-water extraction and alcohol precipitation has the potential to be utilized as an effective potential bio-stimulant with high soil improvement and plant growth promotion potential. The polysaccharide-free residual powdered biomass (PRPB) could potentially be used as a bioactive phytochemical with high antioxidant activities such as DPPH and ABTS radical scavenging activity, and ferric-reducing antioxidant power (FRAP) ability, as well as offering high-efficiency inhibitive effects on cancer cells. Additionally, the polysaccharide-free and phytochemical-free residual powdered biomass (PPRPB) has the potential to be used as a biodiesel feedstock with the required fuel properties. This multiproduct biorefining process represents a promising holistic zero-waste technology for the production of chemicals, food, energy, and feed that is both commercially and industrially feasible.

Supplementary Information The online version contains supplementary material available at https://doi.org/10.1007/s13399-021-02285-0.

Acknowledgements The authors are thankful to the Biodiversity-Based Economy Development Office (Public organization) and National Research Council of Thailand (NRCT) for financial support. This research work was partially supported by Chiang Mai University, Thailand.

Funding The authors are thankful to the Biodiversity-Based Economy Development Office (Public organization) and National Research Council of Thailand (NRCT) for financial support. This research work was partially supported by Chiang Mai University, Thailand.

Declarations

Conflict of interest The authors declare no competing interests.

References

1. Pathak J, Maurya PK, Singh SP, Häder DP, Sinha RP (2018) Cyanobacterial farming for environment friendly sustainable agriculture practices: innovations and perspectives. Front Environ Sci 6:7. https://doi.org/10.3389/fenvs.2018.00007
2. Shahid A, Usman M, Atta Z, Musharraf SG, Malik S, Elkamel A, Shahid M, Alkhattabi NA, Gull M, Mehmood MA (2021) Impact of wastewater cultivation on pollutant removal, biomass production, metabolite biosynthesis, and carbon dioxide fixation of newly isolated cyanobacteria in a multiproduct biorefinery paradigm. Bioresour Technol 333:125194. https://doi.org/10.1016/j.biortech.2021.125194
3. Celis-Plá PS, Rearte TA, Neori A, Masojídek J, Bonomi-Barufi J, Álvarez-Gómez F, Ranglová K, da Silva JC, Abdala R, Gómez C, Caporgno M (2021) A new approach for cultivating the cyanobacterium *Nostoc calcicola* (MACC-612) to produce biomass and bioactive compounds using a thin-layer raceway pond. Algal Res 59:102421. https://doi.org/10.1016/j.algal.2021.102421
4. Facey JA, Apte SC, Mitrovic SM (2019) A review of the effect of trace metals on freshwater cyanobacterial growth and toxin production. Toxins 11:643. https://doi.org/10.3390/toxins11110643
5. Facey JA, Rogers TA, Apte SC, Mitrovic SM (2021) Micronutrients as growth limiting factors in cyanobacterial blooms; a survey of freshwaters in South East Australia. Aquat Sci 83:28. https://doi.org/10.1007/s00027-021-00783-x
6. Silveira SB, Odebrecht C (2019) Effects of salinity and temperature on the growth, toxin production, and akinete germination of the cyanobacterium *Nodularia spumigena*. Front Mar Sci 6:339. https://doi.org/10.3389/fmars.2019.00339
7. Khajepour F, Hosseini SA, Nasrabadi RG, Markou G (2015) Effect of light intensity and photoperiod on growth and biochemical composition of a local isolate of *Nostoc calcicola*. Appl Biochem Biotechnol 176:2279–2289. https://doi.org/10.1007/s12010-015-1717-9
8. Ma R, Lu F, Bi Y, Hu Z (2015) Effects of light intensity and quality on phycobiliprotein accumulation in the cyanobacterium

Nostoc sphaeroides Kützing. Biotechnol Lett 37:1663–1669. https://doi.org/10.1007/s10529-015-1831-3
9. Polyzois A, Kirilovsky D, Dufat TH, Michel S (2020) Effects of modification of light parameters on the production of cryptophycin, cyanotoxin with potent anticancer activity, in *Nostoc* sp. Toxins 12:809. https://doi.org/10.3390/toxins12120809
10. Gour RS, Bairagi M, Garlapati VK, Kant A (2018) Enhanced microalgal lipid production with media engineering of potassium nitrate as a nitrogen source. Bioengineered 9:98–107. https://doi.org/10.1080/21655979.2017.1316440
11. Kostas ET, White DA, Cook DJ (2017) Development of a biorefinery process for the production of speciality chemical, biofuel and bioactive compounds from *Laminaria digitata*. Algal Res 28:211–219. https://doi.org/10.1016/j.algal.2017.10.022
12. Roy M, Mohanty K (2021) Valorization of de-oiled microalgal biomass as a carbon-based heterogeneous catalyst for a sustainable biodiesel production. Bioresour Technol 337:125424. https://doi.org/10.1016/j.biortech.2021.125424
13. Ruangrit K, Chaipoot S, Phongphisutthinant R, Duangjan K, Phinyo K, Jeerapan I, Pekkoh J, Srinuanpan S (2021) A successful biorefinery approach of macroalgal biomass as a promising sustainable source to produce bioactive nutraceutical and biodiesel. Biomass Conv. Bioref. https://doi.org/10.1007/s13399-021-01310-6
14. Waterbury JB, Stanier RY (1981) Isolation and growth of cyanobacteria from marine and hypersaline environments. In Starr MP, Stolp H, Trüper HG, Balows A, Schlegel HG (eds), The Prokaryotes, Vol. 1, Springer-Verlag, Berlin, pp. 247–256. https://doi.org/10.1007/978-3-662-13187-9_9
15. Dubois M, Gilles KA, Hamilton JK, Rebers PT, Smith F (1956) Colorimetric method for determination of sugars and related substances. Anal Chem 28:350–356. https://doi.org/10.1021/ac60111a017
16. Miller GL (1959) Use of dinitrosalicylic acid reagent for determination of reducing sugar. Anal Chem 31:426–428. https://doi.org/10.1021/ac60147a030
17. Tiche S, Issakul K, Ngearnpat N (2018) Efficiency of polysaccharide and *Nostoc* sp. up2 cells on growth of rice seedling (sanpah-twang 1) and soil quality improvement. The 6th International Conference on Biochemistry and Molecular Biology (BMB2018), Thailand. 20–22 June 2018. pp. 1–10.
18. AOAC (1990) Official methods of analysis (15th ed.). Association of Official Analytical Chemists, Washington DC, USA.
19. Gelman F, Binstock R, Halicz L (2012) Application of the Walkley-Black titration for the organic carbon quantification in organic rich sedimentary rocks. Fuel 96:608–610. https://doi.org/10.1016/j.fuel.2011.12.053
20. Doran G, Zander A (2012) An improved method for measuring soil microbial activity by gas phase flow injection analysis. Rev Bras Ciênc Solo 36:349–357. https://doi.org/10.1590/S0100-06832012000200004
21. Rihayat T, Salim S, Arlina A, Fona Z, Jalal R, Alam PN, Sami M, Syarif J, Juhan N (2018) Determination of CEC value (cation exchange capacity) of bentonites from North Aceh and Bener Meriah, Aceh Province, Indonesia using three methods. InIOP Conference Series: Materials Science and Engineering 334:012054.
22. Hartman D (2011) Perfecting your spread plate technique. J Microbiol Biol Educ 12:204–205. https://doi.org/10.1128/jmbe.v12i2.324
23. Rastogi RP, Incharoensakdi A, Madamwar D (2014) Responses of a rice-field cyanobacterium *Anabaena siamensis* TISTR-8012 upon exposure to PAR and UV radiation. J Plant Physiol 171:1545–1553. https://doi.org/10.1016/j.jplph.2014.07.011
24. Pekkoh J, Ruangrit K, Pumas C, Duangjan K, Chaipoot S, Phongphisutthinant R, Jeerapan I, Sawangrat K, Pathom-aree W, Srinuanpan S (2021) Transforming microalgal Chlorella biomass into cosmetically and nutraceutically protein hydrolysates using high-efficiency enzymatic hydrolysis approach. Biomass Conv. Bioref. https://doi.org/10.1007/s13399-021-01622-7
25. Lomakool S, Ruangrit K, Jeerapan I, Tragoolpua Y, Pumas C, Srinuanpan S, Pekkoh J, Duangjan K (2021) Biological activities and phytochemicals profiling of different cyanobacterial and microalgal biomass. Biomass Convers. Biorefin. https://doi.org/10.1007/s13399-021-01974-0
26. Umthong S, Phuwapraisirisan P, Puthong S, Chanchao C (2011) In vitro antiproliferative activity of partially purified *Trigona laeviceps* propolis from Thailand on human cancer cell lines. BMC Complement Altern Med 11:37. https://doi.org/10.1186/1472-6882-11-37
27. Srinuanpan S, Cheirsilp B, Prasertsan P, Kato Y, Asano Y (2018) Photoautotrophic cultivation of oleaginous microalgae and co-pelletization with filamentous fungi for cost-effective harvesting process and improved lipid yield. Aquacult Int 26:1493–1509. https://doi.org/10.1007/s10499-018-0300-0
28. Talebi AF, Mohtashami SK, Tabatabaei M, Tohidfar M, Bagheri A, Zeinalabedini M, Mirzaei HH, Mirzajanzadeh M, Shafaroudi SM, Bakhtiari S (2013) Fatty acids profiling: a selective criterion for screening microalgae strains for biodiesel production. Algal Res 2:258–267. https://doi.org/10.1016/j.algal.2013.04.003
29. Patel A, Sartaj K, Pruthi PA, Pruthi V, Matsakas L (2019) Utilization of clarified butter sediment waste as a feedstock for cost-effective production of biodiesel. Foods 8:234. https://doi.org/10.3390/foods8070234
30. Luo L, Ren H, Pei X, Xie G, Xing D, Dai Y, Ren N, Liu B (2019) Simultaneous nutrition removal and high-efficiency biomass and lipid accumulation by microalgae using anaerobic digested effluent from cattle manure combined with municipal wastewater. Biotechnol Biofuels 12:218. https://doi.org/10.1186/s13068-019-1553-1
31. Fernández-Juárez V, Bennasar-Figueras A, Sureda-Gomila A, Ramis-Munar G, Agawin NSR (2020) Differential effects of varying concentrations of phosphorus, iron, and nitrogen in N_2-fixing cyanobacteria. Front Microbiol 11:541558. https://doi.org/10.3389/fmicb.2020.541558
32. Zabochnicka-Swiątek M, Kamizela T, Kowalczyk M, Kalaji HM, Bąba W (2019) Inexpensive and universal growth media for biomass production of microalgae. Global NEST J 21:82–89. https://doi.org/10.30955/gnj.002558
33. Markou G, Vandamme D, Muylaert K (2014) Microalgal and cyanobacterial cultivation: The supply of nutrients. Water Res 65:186–202. https://doi.org/10.1016/j.watres.2014.07.025
34. Yaakob MA, Mohamed RM, Al-Gheethi A, Ravishankar GA, Ambati RR (2021) Influence of nitrogen and phosphorus on microalgal growth, biomass, lipid, and fatty acid production: an overview. Cells 10:393. https://doi.org/10.3390/cells10020393
35. Marino RW, Howarth R (2014) Nitrogen fixation in freshwater and saline waters. In: Reference Module in Earth Systems and Environmental Sciences, Elsevier, pp 230–257. https://doi.org/10.1016/B978-0-12-409548-9.09402-1
36. Pandey S, Kumar S (2020) Reactive extraction of gallic acid from aqueous solution with Tri-n-octylamine in oleyl alcohol: equilibrium, thermodynamics and optimization using RSM-rCCD. Sep Purif Technol 231:115904. https://doi.org/10.1016/j.seppur.2019.115904
37. Lv H, Xia F, Jia S, Cui X, Yuan N (2015) Effects of K_2HPO_4 on the growth of *Nostoc Flagelliforme* in liquid media with different carbon sources. In Advances in Applied Biotechnology. Springer,

Berlin, Heidelberg. pp. 407–415. https://doi.org/10.1007/978-3-662-45657-6_43
38. Kim HS, Park WK, Lee B, Seon G, Suh WI, Moon M, Chang YK (2019) Optimization of heterotrophic cultivation of Chlorella sp. HS2 using screening, statistical assessment, and validation. Sci. Rep 9:19383. https://doi.org/10.1038/s41598-019-55854-9
39. de Oliveira CY, Viegas TL, da Silva MF, Fracalossi DM, Lopes RG, Derner RB (2020) Effect of trace metals on growth performance and accumulation of lipids, proteins, and carbohydrates on the green microalga *Scenedesmus obliquus*. Aquacult Int 28:1435–1444. https://doi.org/10.1007/s10499-020-00533-0
40. Shetty P, Gitau MM, Maróti G (2019) Salinity stress responses and adaptation mechanisms in eukaryotic green microalgae. Cells 8:1657. https://doi.org/10.3390/cells8121657
41. Mishra A, Mandoli A, Jha B (2008) Physiological characterization and stress-induced metabolic responses of Dunaliella salina isolated from salt pan. J Ind Microbiol Biotechnol 35:1093. https://doi.org/10.1007/s10295-008-0387-9
42. Hiremath S, Mathad P (2010) Impact of salinity on the physiological and biochemical traits of *Chlorella vulgaris* Beijerinck. J Algal Biomass Utln 1:51–59
43. Maneechote W, Cheirsilp B, Srinuanpan S, Pathom-aree W (2021) Optimizing physicochemical factors for two-stage cultivation of newly isolated oleaginous microalgae from local lake as promising sources of pigments, PUFAs and biodiesel feedstocks. Bioresour Technol Rep 25:100738. https://doi.org/10.1016/j.biteb.2021.100738
44. Srinuanpan S, Cheirsilp B, Boonsawang P, Prasertsan P (2019) Immobilized oleaginous microalgae as effective two-phase purify unit for biogas and anaerobic digester effluent coupling with lipid production. Bioresour Technol 281:149–157. https://doi.org/10.1016/j.biortech.2019.02.085
45. de Oliveira CA, Oliveira WC, Ribeiro SM, Stringheta PC, Nascimento AG (2014) Effect of light intensity on the production of pigments in *Nostoc* spp. Eur J Biol Med Sci Res 2:23–36
46. Thawechai T, Cheirsilp B, Louhasakul Y, Boonsawang P, Prasertsan P (2016) Mitigation of carbon dioxide by oleaginous microalgae for lipids and pigments production: effect of light illumination and carbon dioxide feeding strategies. Bioresour Technol 219:139–149. https://doi.org/10.1016/j.biortech.2016.07.109
47. Sirisuk P, Ra CH, Jeong GT, Kim SK (2018) Effects of wavelength mixing ratio and photoperiod on microalgal biomass and lipid production in a two-phase culture system using LED illumination. Bioresour Technol 253:175–181. https://doi.org/10.1016/j.biortech.2018.01.020
48. Lee NK, Oh HM, Kim HS, Ahn CY (2017) Higher production of C-phycocyanin by nitrogen-free (diazotrophic) cultivation of *Nostoc* sp. NK and simplified extraction by dark-cold shock. Bioresour Technol 227:164–170. https://doi.org/10.1016/j.biortech.2016.12.053
49. Wang HB, Wu SJ, Liu D (2014) Preparation of polysaccharides from cyanobacteria *Nostoc commune* and their antioxidant activities. Carbohydr Polym 99:553–555. https://doi.org/10.1016/j.carbpol.2013.08.066
50. Li H, Su L, Chen S, Zhao L, Wang H, Ding F, Chen H, Shi R, Wang Y, Huang Z (2018) Physicochemical characterization and functional analysis of the polysaccharide from the edible microalga *Nostoc sphaeroides*. Molecules 23:508. https://doi.org/10.3390/molecules23020508
51. Shen SG, Lin YH, Zhao DX, Wu YK, Yan RR, Zhao HB, Tan ZL, Jia SR, Han PP (2019) Comparisons of functional properties of polysaccharides from *Nostoc flagelliforme* under three culture conditions. Polymers 11:263. https://doi.org/10.3390/polym11020263
52. Liu X, Zhang M, Liu H, Zhou A, Cao Y, Liu X (2018) Preliminary characterization of the structure and immunostimulatory and anti-aging properties of the polysaccharide fraction of *Haematococcus pluvialis*. RSC adv 8:9243–9252. https://doi.org/10.1039/c7ra11153c
53. Wang L, Liu HM, Qin GY (2017) Structure characterization and antioxidant activity of polysaccharides from Chinese quince seed meal. Food Chem 234:314–322. https://doi.org/10.1016/j.foodchem.2017.05.002
54. Zhong G, Pan W, Huang Z, Guo K, Hu J, Liu P, Chen S, Wang Y, Ai L, Huang Z (2021) Physicochemical and geroprotective comparison of *Nostoc sphaeroides* polysaccharides across colony growth stages and with derived oligosaccharides. J Appl Phycol 33:939–952. https://doi.org/10.1007/s10811-021-02383-6
55. Can HK, Gurbuz F, Odabaşı M (2019) Partial characterization of cyanobacterial extracellular polymeric substances for aquatic ecosystems. Aquat Ecol 53:431–440. https://doi.org/10.1007/s10452-019-09699-z
56. Monsur HA, Jaswir I, Simsek S, Amid A, Alam Z (2017) Chemical structure of sulfated polysaccharides from brown seaweed (*Turbinaria turbinata*). Int J Food Prop 20:1457–1469. https://doi.org/10.1080/10942912.2016.1211144
57. Cruz D, Vasconcelos V, Pierre G, Michaud P, Delattre C (2020) Exopolysaccharides from cyanobacteria: strategies for bioprocess development. Appl Sci 10:3763. https://doi.org/10.3390/app10113763
58. Chamizo S, Rodríguez-Caballero E, Cantón Y, De Philippis R (2018) Soil inoculation with cyanobacteria: reviewing its' potential for agriculture sustainability in drylands. Agri. Res. Tech Open Access. J 18:556046.
59. Chamizo S, Adessi A, Mugnai G, Simiani A, De Philippis R (2019) Soil type and cyanobacteria species influence the macromolecular and chemical characteristics of the polysaccharidic matrix in induced biocrusts. Microb Ecol 78:482–493. https://doi.org/10.1007/s00248-018-1305-y
60. Hanson PJ, Edwards NT, Garten CT, Andrews JA (2000) Separating root and soil microbial contributions to soil respiration: a review of methods and observations. Biogeochemistry 48:115–146. https://doi.org/10.1023/A:1006244819642
61. Rachidi F, Benhima R, Sbabou L, El Arroussi H (2020) Microalgae polysaccharides bio-stimulating effect on tomato plants: growth and metabolic distribution. Biotechnol Rep 25:e00426. https://doi.org/10.1016/j.btre.2020.e00426
62. Santini G, Biondi N, Rodolfi L, Tredici MR (2021) Plant biostimulants from cyanobacteria: an emerging strategy to improve yields and sustainability in agriculture. Plants 10:643. https://doi.org/10.3390/plants10040643
63. Saucedo S, Contreras RA, Moenne A (2015) Oligo-carrageenan kappa increases C, N and S assimilation, auxin and gibberellin contents, and growth in *Pinus radiata* trees. J For Res 26:635–640. https://doi.org/10.1007/s11676-015-0061-9
64. Xu Y, Rossi F, Colica G, Deng S, De Philippis R, Chen L (2013) Use of cyanobacterial polysaccharides to promote shrub performances in desert soils: a potential approach for the restoration of desertified areas. Biol Fertil Soils 49:143–152. https://doi.org/10.1007/s00374-012-0707-0
65. Wakeel A, Jan SA, Ullah I, Shinwari ZK, Xu M (2019) Solvent polarity mediates phytochemical yield and antioxidant capacity of Isatis tinctoria. PeerJ 7:e7857. https://doi.org/10.7717/peerj.7857
66. Tabassum S, Ahmed M, Mirza B, Naeem M, Zia M, Shanwari ZK, Khan GM (2017) Appraisal of phytochemical and in vitro biological attributes of an unexplored folklore: *Rhus Punjabensis* Stewart. BMC Complement Altern Med 17:146. https://doi.org/10.1186/s12906-017-1659-6
67. de Morais MG, Vaz BD, de Morais EG, Costa JA (2015) Biologically active metabolites synthesized by microalgae. Biomed Res. Int 835761. https://doi.org/10.1155/2015/835761

68. Chamnanpuen P, Satitpatipan V, Sirisattha S, Muangman T (2020) Effect of cyanobacteria (*Nostoc* species) extracts on osteogenesis activities. Walailak J Sci Tech 17:620–630. https://doi.org/10.48048/wjst.2020.5350
69. Martins N, Barros L, Ferreira IC (2016) In vivo antioxidant activity of phenolic compounds: facts and gaps. Trends Food Sci Technol 48:1–12. https://doi.org/10.1016/j.tifs.2015.11.008
70. Xu Y, Harvey PJ (2019) Carotenoid production by *Dunaliella salina* under red light. Antioxidants 8:123. https://doi.org/10.3390/antiox8050123
71. Jesumani V, Du H, Pei P, Aslam M, Huang N (2020) Comparative study on skin protection activity of polyphenol-rich extract and polysaccharide-rich extract from *Sargassum vachellianum*. PLoS ONE 15:e0227308. https://doi.org/10.1371/journal.pone.0227308
72. Ijaz S, Hasnain S (2016) Antioxidant potential of indigenous cyanobacterial strains in relation with their phenolic and flavonoid contents. Nat Prod Res 30:1297–1300. https://doi.org/10.1080/14786419.2015.1053088
73. Vega J, Bonomi-Barufi J, Gómez-Pinchetti JL, Figueroa FL (2020) Cyanobacteria and red macroalgae as potential sources of antioxidants and UV radiation-absorbing compounds for cosmeceutical applications. Mar Drugs 18:659. https://doi.org/10.3390/md18120659
74. Yasin D, Zafaryab M, Ansari S, Ahmad N, Khan NF, Zaki A, Rizvi MM, Fatma T (2019) Evaluation of antioxidant and antiproliferative efficacy of *Nostoc muscorum* NCCU-442. Biocatal Agric Biotechnol 17:284–293. https://doi.org/10.1016/j.bcab.2018.12.001
75. Karan T, Aydin A (2018) Anticancer potential and cytotoxic effect of some freshwater cyanobacteria. rop. J Pharm Res 17:2183–2188. https://doi.org/10.4314/tjpr.v17i11.11
76. de Oliveira DT, Vasconcelos CT, Feitosa AM, Aboim JB, de Oliveira AD, Xavier LP, Santos AS, Gonçalves EC, da Rocha Filho GN, do Nascimento LA, (2018) Lipid profile analysis of three new Amazonian cyanobacteria as potential sources of biodiesel. Fuel 234:785–788. https://doi.org/10.1016/j.fuel.2018.07.080
77. Folayan AJ, Anawe PA, Aladejare AE, Ayeni AO (2019) Experimental investigation of the effect of fatty acids configuration, chain length, branching and degree of unsaturation on biodiesel fuel properties obtained from lauric oils, high-oleic and high-linoleic vegetable oil biomass. Energy Rep 5:793–806. https://doi.org/10.1016/j.egyr.2019.06.013
78. Cheirsilp B, Srinuanpan S, Mandik YI (2020) Efficient harvesting of microalgal biomass and direct conversion of microalgal lipids into biodiesel. In Microalgae Cultivation for Biofuels Production, Academic Press. pp. 83–96. https://doi.org/10.1016/B978-0-12-817536-1.00006-0
79. Jawaharraj K, Karpagam R, Ashokkumar B, Pratheeba CN, Varalakshmi P (2016) Enhancement of biodiesel potential in cyanobacteria: using agro-industrial wastes for fuel production, properties and acetyl CoA carboxylase D (accD) gene expression of *Synechocystis* sp. NN Renew Energy 98:72–77. https://doi.org/10.1016/j.renene.2016.02.038
80. Ali BA, Indabawa II, Yaro CA, Opisa AN (2019) Production and characterization of biodiesel from the microalga, *Chlorella vulgaris* (Beijerinck 1890). Trends Appl Sci Res 14:90–97. https://doi.org/10.3923/tasr.2019.90.97
81. Karpagam R, Raj KJ, Ashokkumar B, Varalakshmi P (2015) Characterization and fatty acid profiling in two fresh water microalgae for biodiesel production: lipid enhancement methods and media optimization using response surface methodology. Bioresour Technol 188:177–184. https://doi.org/10.1016/j.biortech.2015.01.053
82. Sivaramakrishnan R, Incharoensakdi A (2017) Enhancement of total lipid yield by nitrogen, carbon, and iron supplementation in isolated microalgae. J Phycol 53:855–868. https://doi.org/10.1111/jpy.12549
83. Sharma AK, Sharma A, Singh Y, Chen WH (2021) Production of a sustainable fuel from microalgae *Chlorella minutissima* grown in a 1500 L open raceway ponds. Biomass Bioenerg 149:106073. https://doi.org/10.1016/j.biombioe.2021.106073
84. Dwivedi G, Sharma MP (2014) Potential and limitation of straight vegetable oils as engine fuel–an Indian perspective. Renew Sust Energ Rev 33:316–322. https://doi.org/10.1016/j.rser.2014.02.004
85. Verma P, Sharma MP, Dwivedi G (2016) Impact of alcohol on biodiesel production and properties. Renew Sust Energ Rev 56:319–333. https://doi.org/10.1016/j.rser.2015.11.048
86. Mandik YI, Cheirsilp B, Srinuanpan S, Maneechote W, Boonsawang P, Prasertsan P, Sirisansaneeyakul S (2020) Zero-waste biorefinery of oleaginous microalgae as promising sources of biofuels and biochemicals through direct transesterification and acid hydrolysis. Process Biochem 95:214–222. https://doi.org/10.1016/j.procbio.2020.02.011
87. Ichihara KI, Fukubayashi Y (2010) Preparation of fatty acid methyl esters for gas-liquid chromatography [S]. J Lipid Res 51:635–640. https://doi.org/10.1194/jlr.D001065
88. Nayak M, Swain DK, Sen R (2019) Strategic valorization of de-oiled microalgal biomass waste as biofertilizer for sustainable and improved agriculture of rice (*Oryza sativa* L.) crop. Sci Total Environ 682:475–484. https://doi.org/10.1016/j.scitotenv.2019.05.123